INVESTIGATION OF AN INSTABILITY PHENOMENA OCCURRING IN SUPERSONIC DIFFUSORS

Thesis by

Leo Stoolman

In Partial Fulfillment of the Requirements

For the Degree of

Doctor of Philosophy

California Institute of Technology

Pasadena, California

1953

ACKNOWLEDGMENTS

The author wishes to express his most sincere thanks to Dr. Richard E. Edwards of the Hughes Aircraft Company for his valuable advice on the theoretical aspects of the research; and to Dr. Henry Nagamatsu for his help and advice in planning and carrying out the experimental phase of the research, and interpretation of the phenomena.

Grateful appreciation is also given to Dr. H. S. Tsien for his many valuable suggestions.

The author also wishes to thank Mrs. Betty Wood for the fine drawings contained herein. He would in particular like to thank Mrs. Gerry Van Gieson for the excellent job of typing this manuscript. Also, the skillful construction of the small models by William Sublette is appreciated.

Finally, the author expresses his sincere thanks to the California Institute of Technology and the Hughes Aircraft Company for financial assistance in helping pursue his studies.

SUMMARY

Experimental investigations of supersonic normal shock type diffusors have shown the existence of self-excited oscillations that occur as the internal mass flow is reduced somewhat below its maximum value. There is a lower bound of free stream Mach number (of the order of 1.8) below which no instability could be observed. However, as the free stream Mach number was increased above this lower bound, instability occurred at increasing values of the internal mass flow. Also, the frequency at instability was of the order of the natural frequency of the internal duct acting as an organ pipe.

First-order theoretical investigations of the above phenomena indicate that the instability may (in part) be interpreted as intrinsic, that is, independent of viscous effects at the duct inlet or within the diffusor. The fundamental cause of the instability is shown to be due to the nature of the oscillatory inlet flow conditions that occur as a consequence of the external compression from the shock wave to the inlet, and the type of reflections suffered at the shock wave by upstream traveling pressure waves.

TABLE OF CONTENTS

TABLE OF FIGURES

SYMBOLS

Geometric (Refer to Figs. 3 and 6)

D_1, D_2, etc.	denotes particular diffusor configuration	(Cf. Fig. 3)
θ	diffusor internal expansion angle	" " "
L	diffusor length	" " "
ℓ	length of diffusor plus plenum chamber	" " "
d_3	diffusor inlet diameter	" " "
d_4	diffusor exit diameter	" " "
A	cross sectional area of stream tube entering diffusor	(Cf. Fig. 6)
x_e	throttle position number measured from fully closed value (must be correlated with corresponding mass flow)	
x	coordinate parallel to diffusor axis (positive direction is downstream)	
r	radial coordinate perpendicular to diffusor axis (positive direction is outward from diffusor axis)	
z	coordinate along streamline dividing internal and external flows	
m	slope of above streamline	
R	radius to extremity of stream tube entering the diffusor	

Aerodynamic and Kinetic

U, V	instantaneous velocity components in x, r directions respectively
P	instantaneous pressure

ρ	instantaneous density
R_g	gas constant
c_p	specific heat at constant pressure
γ	ratio of specific heat at constant pressure to that at constant volume
$H = p/\rho^\gamma = e^{\Delta S}$	
S	instantaneous entropy
t	time
u, v	steady state velocity components in x, r directions respectively
y	u/u_2
P	steady state pressure
ρ	steady state density
T	steady state temperature
h	steady state H
a	steady state speed of sound
M	steady state axial Mach number $(M = u/a)$
ξ	shock wave velocity
ω	frequency (radians/sec.)
f	frequency (cycles/sec. or cps)
α	complex frequency = $\lambda + i\omega$
β	reduced frequency = $\omega / \frac{du}{dx}$
G	density transfer function = $(\rho'/\rho)/(u'/u)$
I	entropy transfer function = $(h'/h)/(u'/u)$
τ_1	isentropic wave characteristic length
τ_2	entropy wave characteristic length
λ_w	wave length

i	$\sqrt{-1}$
e	naperian log base

Superscripts and Subscripts

$( )_1$	free stream (Cf. Fig. 6)
$( )_2$	diffusor stream tube station 2 (Cf. Fig. 6)
$( )_3$	diffusor stream tube station 3 " " "
$( )_4$	diffusor stream tube station 4 " " "
$( )_5$	diffusor stream tube station 5 " " "
$( )^*$	diffusor stream tube station * " " "
$( )_s$	stagnation conditions
$( )'$	non-steady perturbations about steady state values
$\overline{( )}$	space average value

I. INTRODUCTION

A. General

The broad objective of this research was the investigation of an instability phenomenon associated with supersonic diffusors in which as the mass flow is reduced below some critical value, the steady state flow breaks down and self excited oscillations occur. The major part of the investigation was experimental, for which the 2.5 inch Supersonic Wind Tunnel facilities of the Guggenheim Aeronautical Laboratory were utilized. In addition, the resulting data were utilized to formulate a phenomenological model for theoretical investigations; and initial analyses have been carried out.

An essential component of an air-breathing engine such as a Ramjet or Turbo-jet is its aerodynamic diffusor, the function of which is to admit free stream air and to convert its kinetic energy to pressure at the diffusor exit (or burner inlet). A measure of the efficiency of the kinetic energy conversion can be expressed as the ratio of stagnation pressures at the diffusor exit and free stream, respectively. Also, for a Ramjet, it can be shown that the thrust is almost directly proportional to the diffusor efficiency. In the subsonic free stream regime the diffusor efficiencies are close to 100%, the only losses suffered being due to internal viscous effects. However, at supersonic free stream speeds the significant efficiency losses are caused by the presence of shock waves (either internal or external) since the incoming air must be slowed down to low subsonic speeds. The attendant entropy increase across such shock waves manifests itself as a decrease in stagnation pressure. Another distinguishing feature of a diffusor operating at

supersonic speeds, as contrasted to subsonic operation, is the presence of self excited oscillations that may occur as the incoming mass flow is reduced below its peak value.

Intensive investigations (Refs. 1, 3, and 11) of the stable regime of supersonic diffusors for various geometric configurations have been carried out in an attempt to reduce the shock wave losses. However, although the occurrence of unstable flow has been acknowledged by some investigators (Refs. 1 and 3), very little further work has been done. The presence of unstable flow which manifests itself as pressure and mass flow pulsations at the burner inlet may have serious detrimental effects on the combustion process. Consequently, a thorough understanding of the conditions leading to instability is necessary in order that appropriate corrective measures be taken. Along with this, it is essential to ascertain if the instability is intrinsic to a system consisting of a duct (internal diffusor) in the presence of shock waves at the inlet irrespective of viscous effects*, or if it is a combination of shock wave and viscous effects.

B. Description of Instability Phenomena and Results of Previous Investigations

Perhaps the most significant development of high efficiency supersonic diffusors was originally done by Oswatitsch (Ref. 1), and further developed by Ferri (Ref. 11) in this country and Lukasiewiz (Ref. 3) in England. The method of operation of a supersonic diffusor in the stable flow regime, illustrating transition to instability, can best be

---

* By viscous effects are meant large scale flow separations within the diffusor.

described by presenting Oswatitsch's results.

The pertinent results of Ref. 1 are reproduced in Figs. 1 and 2. A scale drawing of the diffusor is shown in Fig. 1. The diffusor consists of an inner body with a protruding 40° cone followed by a truncated cone just before the inlet, and an annular internal diffusor. The internal duct was terminated by a throttle aft of the diffusor exit, the opening of which could be adjusted so as to vary the mass flow. This type of diffusor achieves its high efficiency by allowing external compression through a series of oblique shocks, and finally through a normal shock at a reduced Mach number. The resulting stagnation pressure achieved is significantly higher than that obtained behind a normal shock at free stream speeds. The performance results are shown in Fig. 2a, in terms of diffusor efficiency, P_{as}/P_s, and relative mass flow, A/A_e, as a function of throttle opening. For the throttle open wide (i.e., A_o/A_e large), there is supersonic flow into the inlet and the consequent occurrence of an internal normal shock. As A_o/A_e decreases, the internal normal shock moves upstream towards the inlet, and the efficiency increases, but the mass flow remains constant. When the normal shock is just at the inlet the efficiency reaches its maximum value, and upon further decreasing the throttle opening the normal shock wave moves out ahead of the inlet. There it merges with the protruding tip conical shock, and the mass flow starts to decrease. The constant mass flow regime is denoted as super critical, and the reduced mass flow regime as sub-critical. Oswatitsch found that as the mass flow was reduced slightly below critical, the pressure recovery and mass flow took a sudden drop. In the remainder of the sub-critical regime the data appeared erratic and difficult to duplicate. Observation of spark schlieren photographs (exposure = 10 microseconds) of the inlet flow

region indicated that the flow was non-steady, and the entire inlet shock configuration was undergoing violent pulsations. In Fig. 2b, sketched reproductions of the above photographs are shown which illustrate the transition from stable to unstable flow. For the latter, the limits of shock wave movement are indicated, and the photographs also show a concomitant boundary layer separation, associated with the instability. Other than the above photographs, no attempts were made to make any additional measurements than to note that a characteristic noise of low frequency accompanied the instability.

Rough exploratory tests of a diffusor which was practically identical to Oswatitsch's were made in the JPL 12" tunnel at Mach numbers of 1.8 up to 2.5, and again the instability was noted when operation in the subcritical regime was attempted. As the Mach number was increased, the extent of the stable subcritical regime was further reduced, until at a Mach number of 2.5 no stable subcritical flow could be achieved. In all cases the observed frequency was fairly regular, but significantly lower than one would calculate assuming that the internal diffusor acted as an organ pipe (i.e., a frequency corresponding to a $\frac{1}{4}$ wave length). However, upon further closing the throttle corresponding to the mid sub-critical range, an increase in frequency equal approximately to that of the organ pipe was noted.

Thus, the above investigations have indicated that a self excited oscillation can exist for diffusors operating at supersonic speeds. For a given diffusor the stability limits are a function of free stream Mach number and mass flow. That is, as the mass flow is reduced somewhat below the diffusor critical point, there is a transition from steady flow to self excited oscillations. The mechanism which enables the

diffusor duct system to absorb energy from the free stream is linked to the presence of the detached shock waves and possible shock wave boundary layer interaction since these are the distinguishing features of a diffusor operating at supersonic speeds as contrasted to operation in the subsonic free stream regime. An analogous phenomenon in which a system becomes unstable by absorbing energy from the free stream is that encountered in the airplane flutter problem. That is, a vibrating system such as a wing aileron combination, which has more than one degree of freedom can become unstable as the airplane speed is increased to a point wherein small initial displacements of components of the system increase exponentially with time due to the equality of the natural frequency of the aileron and wing.

C. Other Examples of Self-Excited Oscillations Occuring in Aerodynamic or Aero-Thermodynamic Systems

1. Hartmann Sound Generator

This device, the phenomena of whichwere first discovered in 1931, is reported in Ref. 2, and its physical and performance characteristics are summarized in Fig. 19. In essence, an organ pipe with the open end pointing upstream is inserted into a supersonic stream issuing from a choked orifice. The jet chamber pressure is substantially higher than that required to produce M = 1 at the orifice, so that further expansion exists in the jet stream, and the characteristic wavy jet is produced as originally explained by Prandtl in Ref. 12. The pitot stagnation pressure*

---

* This corresponds to the stagnation pressure behind a normal shock.

along the jet axis was measured, and the corresponding Mach number distributions are shown in Fig. 19. As the organ pipe inlet was inserted into the jet near the orifice where M = 1, no instability was observed, but as it was moved down stream where M > 1, instability occurred and the inlet normal shock wave oscillated between the limits as shown. The frequencies emitted were measured with a Kundt's tube and corresponded to the length ($\ell + \ell_0$) being a quarter wave length, which corresponds to the natural frequency of an organ pipe. Instabilities were observed over a wide range of organ pipe lengths, and similar results were obtained using a Helmholtz Resonator. With the organ pipe resonator it was possible, by making ℓ sufficiently small, to attain frequencies of the order of 200,000 cycles per second. Also, the energy of the sound being radiated from the tube was of the order of 10 - 20% of the energy in the supersonic jet stream. This makes a fairly efficient sound producing device, but indicates that a significant amount of energy available from the free stream is going into pulsating motion.

2. Liquid Rocket Motors

The liquid rocket motor is an aero-thermodynamic system in which a liquid fuel is injected at the front end of a chamber, combines chemically with an oxidizer producing a high temperature gas, and expands through a nozzle at the aft end of the chamber. As the fuel flow is increased above a critical value, high frequency self excited oscillations are observed of the order of magnitude of the natural acoustic frequency of the chamber.

In Crocco's analysis of rocket motor instability (Ref. 6), it

is shown that a pressure sensitive fuel feeding is not a necessary mechanism for producing self-excited oscillations. Rather they can be caused by interactions between pressure oscillations set up by wave motions within the chamber and reflected from the nozzle end, and which are in turn reinforced by pressure oscillations at the injection end. This reeinforcement is due to the time lag that exists in producing a gas from the liquid fuel which allows the injection end oscillations to be approximately in phase with the gas chamber oscillations. The instability described by Crocco is inherent to the system irrespective of the type of fuel feeding, and in that respect it has been called intrinsic.

D. Research Program

Further exploratory tests of the Oswatitsch diffusor were made in which the inner body was removed so as to reduce the severe viscous separation effects noted on the cone preceding instability. When this was done, instability was still observed but at a lower mass flow (about 50% of the maximum), and the self-excited oscillations persisted from there on to complete closure of the throttle.

Thus, it appeared that instability could occur even in the absence of severe viscous effects, and that the self-excited oscillations produced could be of an intrinsic nature. That is, there is the possibility that such oscillations are primarily a function of the duct acting as a resonator and through the medium of a detached inlet shock wave, a mechanism is created by which energy can be absorbed from the free stream to maintain the resonator oscillations.

Based on the above exploratory investigation, it was felt that a

thorough understanding of the open nose diffusor* instability, in particular the determination of whether such an instability is intrinsic, would be a proper first step in attempting to understand the corresponding phenomenon of the Oswatitch type diffusor. The latter is further complicated by the presence of shock induced boundary layer separation that may be an additional mechanism capable of inducing self excited oscillations.

Consequently, the objectives for the research program were set as follows:

(1) Diffusor Type: Open nose diffusor configurations having small internal losses due to viscous effects were selected.

(2) Experimental Program: Experimental investigations were to be made in the 2.5" GALCIT supersonic tunnel over a range of geometric and aerodynamic parameters to determine the pertinent parameters or combinations that lead to instability. An additional objective was the measurement of the necessary aerodynamic parameters just preceding instability so as to help in formulating an appropriate theoretical model of the phenomena.

(3) Theoretical Investigation: The following approach was decided upon, (a) development of a stability criterion as a function of inlet and exit conditions that would establish a quantitative measure for the parameters necessary for instability, (b) set up of a phenomenological model, and

---

* Commonly referred to as a normal shock diffusor.

check to see if the instability phenomena can be explained in whole or in part as intrinsic using the method of small perturbations about the steady state conditions just preceding instability.

II. EXPERIMENTAL INVESTIGATION

A. Test Facilities

The 2.5 inch supersonic wind tunnel of the Guggenheim Aeronautical Laboratory was utilized for all the experimental investigations, and the details of its operation, and associated optical equipment are described in Ref. 14. Briefly, it has a working section 2.5 in. x 2.5 in. in cross section and is capable of achieving Mach numbers from about 1.2 to 4.5. Also, at a free stream Mach number of 2.0, the Reynolds number range is from about 2×10^5 to 10^6 per inch.

The maximum model diameter was selected on the basis of the minimum desirable operating Mach number, and the physical size commensurate with achieving the necessary internal equipment for measurements of internal velocity and pressure distributions. From consideration of the latter, it was felt that a minimum allowable diameter was about 0.5 in., which allowed (from tunnel blocking considerations) a minimum operating Mach number of 1.5.

Internal instrumentation consisted of a total head rake of five 0.031 in. diameter hypodermic needle tubes, and two static orifices located at the diffusor exit. A multi-tube liquid manometer was used for pressure measurements. A sketch of the model is shown in Fig. 3. Various diffusors could be connected to the plenum chamber, and the mass flow was varied by adjusting the exit plug which formed a sonic throat. The exit plug was connected to a rack and pinion gear positioning device, and was adjustable from outside the tunnel. The mass flow calibration of the exit throttle plug was done by integrating the velocity and

density distributions measured at the diffusor exit as a function of plug position. A sketch of the model installed in the tunnel is shown in Fig. 4.

The small size of the model prohibited using any instantaneous type pressure gages for non-steady flow measurements. However, since the onset of instability could be detected by observations of shock wave motion, a schlieren strobotac system was devised, a sketch of which is shown in Fig. 5. A 10 inch diameter strobo-wheel having 20 slot cutouts was inserted just above the condenser lense and slit. The strobo-wheel was driven by a D.C. motor, the speed of which could be controlled by a Variac. When the wheel was in motion, the light source could be interrupted at various frequencies depending upon the motor speed. Top frequencies of the order of 1500 cps could be measured. The wheel speed was determined by a neon strobotac. For instability determination the schlieren strobotac was set at a fairly high frequency so that practically any minute movement of the shock wave could be detected as the mass flow was reduced to the instability point. Without the schlieren strobotac, it was difficult to notice the onset of instability until a fairly large amplitude movement had built up. At the diffusor mass flow where the oscillation became steady, the light source frequency was adjusted until the shock wave movement was stopped, at which point the frequency was measured.

Instability observations were also made with a shadowgraph system, in which the slit was replaced by a pin-hole aperture, and viewing was done on a ground glass screen placed over the wind tunnel window.

Photographic observations of the non-steady inlet shock wave were

made using long exposure* photographs (1/50 sec.). The limits of shock position could be detected since the period of the oscillations were substantially less than the above exposure time so that the region traversed by the shock wave showed up as a multi-exposure (Cf. Fig. 14b). In addition, many spark exposure** photographs (10 micro seconds) were taken which yielded a series of single exposure photographs showing the shock wave in various positions of its travel during a cycle (Cf. Fig. 14c).

B. Diffusor Models

As pointed out in Section I, the experimental phase of the research was to be devoted to the open nose type of diffusor.

In order to keep the geometry simple, it was decided to use conical diffusors having an internal diffusion angle of 10°. This is in accord with wind tunnel and subsonic diffusor practice of keeping viscous separation losses low. A series of models having expansion ratios A_3/A_4 varying from 0.28 to 0.51 was selected as sufficient for covering the range encountered in the subsonic regime of most ramjet or turbojet diffusors. In addition a "diffusor" having no internal diffusion, i.e., just a straight pipe, was also investigated to check the effect on stability of zero axial velocity gradient. A sketch of the above diffusor models is shown in Fig. 3. The diffusor inlet lip was merely the termination of the truncated cone forming the diffusor, and its

---

* Referred to as steady exposure.

** Referred to as flash exposure.

thickness was made as small as possible commensurate with negligible structural deformation.

The length of the plenum chamber shown in Fig. 3 was selected on the basis of achieving reasonably low frequencies of self-excited oscillations commensurate with that of the available frequency measuring equipment. However, before this length was fixed, exploratory tests were made to determine its effect on stability. Using diffusor D_2, a series of tests were made at $M_1 = 2.0$ with plenum chamber lengths varying from 0.5 to 2.75 in. For all the lengths checked, instability occurred at approximately the same internal mass flow, the only difference being in the resulting self-excited oscillation frequency which varied inversely with diffusor plus plenum chamber length, as one should expect.

C. Discussion of Results

1. Nomenclature

Refer to the list of symbols on page viii, and model sketch in Fig. 6. Fig. 6 shows typical inlet conditions for flow in the sub-critical regime. The various stations indicated by encircled numbers are defined as follows:

(1) -- free stream

(2) -- just down stream of detached shock wave

(3) -- diffusor inlet

(4) -- diffusor exit

(5) -- plenum chamber exit

(*) -- choked exit throttle

The various regimes are defined as:

(2) to (3) -- external diffusion regime (subcritical)

(3) to (4) -- internal diffusion regime

(4) to (5) -- constant velocity regime

2. Effect of Free Stream Mach Number and Reynolds Number

Tests were carried out for discrete free stream Mach numbers of M_∞ = 1.6, 2.0, 2.4 for each of the diffusors of Fig. 3. At M_∞ = 1.6 no instability could be detected down to zero mass flow. For M_∞ = 2.0 and 2.4 instability was detected, and the trend with Mach number is shown in Fig. 18 where results for diffusor D_2 are illustrated as a stability boundary, i.e., in terms of relative mass flow (A/A_3) * or diffusor exit Mach number, M_4, at instability as a function of free stream Mach number, M_∞. Because of the minimum number of data points, no detailed trend could be established. However, qualitatively the effect of increasing free stream Mach number is seen to aggravate the stability of the system in that larger mass flows are necessary to establish stability.

The remainder of the test program was devoted to investigate only at M_∞ = 2.0 since instability for all the diffusors occurred there, and also a greater stable external regime could be obtained. This enabled easier interpretation of the flow details in the vicinity of the shock wave from the schlieren photographs.

In addition, if one considers the Oswatitsch diffusor of Fig. 1, the surface Mach number = 2.0 at M_∞ = 2.6. Thus, if the cone boundary layer could be removed by some suction device, the resulting inlet

---

* Relative mass flow is defined as the ratio of the actual to the maximum possible mass flow capable of entering the diffusor.

conditions would be essentially the same as for the models of this experiment.

For the majority of the tests, the Reynolds number based on diffusor length was 3.4×10^5 at $M_1 = 2.0$. No significant effect on stability could be detected as the Reynolds number was increased to twice the above value.

3. Effect of Diffusor Geometry

For each of the conical diffusors tested for which the area ratio varied from $A_3/A_4 = 0.28$ to 1.0, instability was detected.

The results in terms of the relative mass flow ratio, A_1/A_3, as a function of A_3/A_4 are shown in Fig. 7. The dotted curves bracket the range of estimated accuracy.

The absolute mass flow is $\rho_1 u_1 A_1 = \rho_1 u_1 A_4 \left(\frac{A_1}{A_3}\right)\left(\frac{A_3}{A_4}\right)$, and from the results of Fig. 7, it is seen that this value remains approximately constant with diffusor area ratio.

4. Diffusor Performance: Transition to Instability

Since the performance of each of the diffusors tested was similar as regards the transition to instability, only the detailed results for diffusors D_2 and D_5 will be presented. The area ratio, A_3/A_4, for diffusor D_2 corresponds roughly to the internal diffusion of the Oswatitsch diffusor of Fig. 1; whereas $A_3/A_4 = 1$ for D_5, represents no internal diffusion.

The experiment consisted of starting with the exit throttle sufficiently wide open so that the diffusor flow remained stable. As the throttle was gradually closed, data consisting of diffusor exit Mach

number profile, pressure, and inlet flow schlieren photographs were obtained, up to the point where instability occurred, and from there on to complete closure of the exit throttle.

The independent variable for all data presented is throttle position, x_e. The units of x_e represent divisions on the throttle positioning wheel and in themselves have no meaning. However, in the stable regime the mass flow increases monotonically with x_e, and in the unstable region the time averaged value of mass flow increases monotonically with x_e up to the critical (or maximum mass flow) point.

Results for Diffusor D_2

Schlieren photographic results are presented in Fig. 14. Fig. 14a is a steady exposure showing stable flow at $x_e = 13$ $(A_1/A_3 = 0.42)$, just preceding instability. As x_e was reduced below $x_e = 13$, instability occurred as manifested by intermittant pulsations of the inlet shock which gradually increased in amplitude and frequency until finally, at $x_e = 8$, a steady frequency of 740 cps was observed. The natural acoustic frequency of the internal duct acting as a one quarter wave length resonator is 900 cps. The frequency remained constant, but the amplitude increased as x_e was further reduced. Fig. 14b is a long exposure photograph, taken at $x_e = 7$, and the steady oscillating shock wave shows up as a multi-exposure as indicated by the greatly thickened "shock wave" when compared to Fig. 14a. The limits of the shock wave movement can also be observed. Figs. 14c-f are a series of flash exposure photographs taken at $x_e = 7$, and they show the shock wave in a series of positions ranging between the aft and forward limits during an oscillation cycle. Figs. 14g-j are

similar results for $x_e = 0$, where steady and flash exposures show the enlarged shock wave movement; and the frequency remained at 740 cps.

Internal performance data are presented in Fig. 8 as stagnation pressure recovery, P_{t_4}/P_{t_0}, relative mass flow A_1/A_3, and average Mach number $\bar{M}_4$ as a function of throttle position, x_e. The significant result to note is that the pressure recovery over practically the entire subcritical range is within a few per cent of the theoretical value, which assumes only a normal shock loss. Thus, the flow in the diffusor is practically isentropic, and shows no evidence of boundary layer separation.

The velocity profiles at the diffusor exit are shown in Fig. 9, as x_e was reduced to instability. The profiles are fairly flat within the measureable range of the instrumentation. This again indicates no severe boundary layer effects, and also that the flow is essentially one dimensional.

To get some idea of the magnitude of axial velocity gradients, the flow was assumed quasi-one dimensional over the internal stream tube from the shock wave to the exit nozzle. The results are shown in Fig. 10. The significant result to note is the extreme gradient in the external diffusion region, due primarily to the close proximity of the inlet shock wave.

Results for Diffusor D_5

Schlieren photographic results are shown in Fig. 15. Fig. 15a shows inlet flow conditions just preceding instability at $x_e = 13$ $\left(A_1/A_3 = 0.16\right)$. For $x_e < 13$, instability occurred as shown in Figs. 15b-d. The observed steady frequency was 870 cps, whereas the natural

acoustic frequency of the internal duct acting as a quarter wave length resonator is 900 cps, and it remained constant down to $\alpha = 0$. Results for $\alpha = 0$ are shown in Figs. 15e-h. Qualitatively, the inlet flow results are similar to those obtained for diffusor D_2. The only significant difference seems to be in the smaller shock wave oscillation amplitude for D_5 as compared to D_2.

Internal performance data for $M = 2.0$ are shown in Figs. 11, 12, and 13, and these show essentially the same results as obtained for diffusor D_2 as regards pressure recovery and velocity profiles.

Inlet Conditions Just Preceding Instability

The characteristics of the external diffusion region, regarding both its size and the shape of the detached shock wave, were obtained for diffusors D_2 and D_5 by enlargements of the above schlieren photographs, at flow conditions just preceding instability. Scale drawings of the pertinent results are shown in Figs. 16 and 17 for D_2 and D_5 respectively. Approximate values of the streamline separating the internal and external flows, and sonic line are indicated.

5. Summary of Results

For the family of conical open nose diffusors investigated, the following are the pertinent results:

(a) Instability can occur over a wide range of diffusor area ratios $\left(A_3/A_4 = 0.28 \text{ to } 1.0 \right)$, as the absolute mass flow is reduced below a critical value that is common to each area ratio. However, in terms of the relative mass flow, A_1/A_3, which is the significant mass flow measure for a diffusor, the effect of increasing the area ratio causes

instability to occur at increasing values of A_1/A_3 .

(b) There is a minimum free stream Mach number ($M_1 = 1.8$) below which no instability was observed over the entire sub-critical range. However, as M_1 was increased, instability occurred at increasing values of the relative mass flow.

(c) The resulting steady shock wave frequency that occurs as the mass flow is reduced below the first occurrence of instability is of the order of magnitude of the natural acoustic frequency of the internal duct acting as an organ pipe (i.e., one quarter wave length).

(d) The flow within the diffusor in the stable regime just prior to instability shows no significant effects of viscous separation, and may be adequately represented by quasi-one dimensional inviscid flow.

(e) The detached shock wave just prior to instability at $M_1 = 2.0$ is slightly curved in the region corresponding to the magnitude of the inlet area. At the extremity of this region the shock wave angle is approximately 75°, and the corresponding flow deflection is about 19°.

(f) The above results (a and b) are in accord with those observed for the Hartmann Sound Generator of Ref. 2.

III. ANALYTIC INVESTIGATION

A. Introduction

The objective of this section is to attempt a quantitative interpretation of the instability phenomena described in Section II in which a steady flow breaks down into a self excited oscillation. The first objective is the development of a stability criterion as a function of the inlet and exit conditions of the internal duct (i.e., diffusor plus plenum chamber) that will establish a quantitative measure for the parameters necessary for instability.

Since the above results show that the inlet conditions are crucial in causing the instability, the remainder of the investigation will be devoted to the analysis of the non-stationary flow phenomena in the external diffusion regime. Since the flow in this region is extremely complicated by virtue of its geometry and possible presence of viscous effects in the neighborhood of the inlet lip, only a first approximation analysis will be attempted for which a phenomenological model is postulated that assumes an inviscid fluid. These, then, are the conditions necessary for ascertaining whether the instability is intrinsic in nature, either in whole or in part.

Since the primary interest is concerned with the onset of instability, it seems appropriate to consider the behavior of small perturbations of the flow parameters about a steady state, and in particular to investigate the growth with time of initial periodic disturbances of the above parameters. Consequently, the equations of motion can be linearized in terms of the perturbations.

As regards most linear instability phenomena, a continuous growth

of the perturbations with time exists, and when the latter get large enough so as to violate the linearizing assumptions, the results no longer apply to this regime. For this regime the methods of non-linear analysis as carried out in Ref. 15 might be used. The experimental results of Section II show that the instability manifested in terms of the inlet shock wave motion builds up to a steady large amplitude (but finite) motion as the mass flow is further reduced from the initial instability point. The phenomena in this regime exhibit an analogous behavior to that associated with "limit cycles" of non-linear systems described in Refs. 15 and 16. The analysis of this phase of the instability phenomena is beyond the scope of the present investigation. However, it is felt that the linear instability is a necessary criterion to explain the phenomenon of breakdown of steady flow.

B. Stability Criteria: General Treatment

1. Introduction

The flow between the diffusor inlet, (3), and the plenum chamber exit, (5), is considered and the boundary conditions at (3) and (5) are kept general. Also, an arbitrary axial distribution of duct cross sectional area is maintained. From the experimental results of Section II, it is concluded that conditions within the internal duct can be appropriately represented by an inviscid quasi-one dimensional flow.

2. Equations of Motion

Based on the above assumptions the equations of motion are:

$$\frac{\partial \bar{u}}{\partial t} + \bar{u}\frac{\partial \bar{u}}{\partial x} = -\frac{1}{\bar{\rho}}\frac{\partial \bar{p}}{\partial x} \qquad \text{(momentum)} \qquad (1)$$

$$A\frac{\partial \bar{\rho}}{\partial t} + \frac{\partial(\bar{\rho}\bar{u}A)}{\partial x} = 0 \qquad \text{(continuity)} \qquad (2)$$

$$\left(\frac{\partial}{\partial t} + \bar{u}\frac{\partial}{\partial x}\right)H = 0 \qquad \text{(energy)} \qquad (3)$$

where $H = \frac{p}{\rho^{\gamma}} = e^{S}$, and henceforth will be referred to as the entropy in place of using e^{S}.

$$p/\rho = R_g T \qquad \text{(state)} \qquad (4)$$

Now, introducing perturbation quantities

$$\begin{aligned} \bar{u} &= u + u' \\ \bar{p} &= p + p' \\ \bar{\rho} &= \rho + \rho' \\ H &= h + h' \end{aligned} \qquad (5)$$

where the unprimed quantities are the steady state values and are only a function of x, and the primed quantities are the non-steady perturbations and are a function of both x and t.

The following are the set of relations governing the steady state flow:

$$\begin{aligned} u\frac{du}{dx} &= -\frac{1}{\rho}\frac{dp}{dx} \\ \frac{d(\rho u A)}{dx} &= 0 \\ dh/dx &= 0 \end{aligned} \qquad (6)$$

Substituting Eqs. (5) and (6) into Eqs. (1) through (3), and retaining only first order terms, the following set of linearized equations of motion are obtained:

$$\frac{\partial}{\partial t}\left(\frac{u'}{u}\right)+u\frac{\partial}{\partial x}\left(\frac{u'}{u}\right)+\frac{p}{\rho u}\frac{\partial}{\partial x}\left(\frac{p'}{p}\right)+\left\{\frac{\rho'}{\rho}-\frac{p'}{p}+2\frac{u'}{u}\right\}\frac{du}{dx}=0 \qquad \text{(momentum)} \qquad (7)$$

$$\frac{\partial}{\partial t}\left(\frac{\rho'}{\rho}\right)+u\left\{\frac{\partial}{\partial x}\left(\frac{u'}{u}\right)+\frac{\partial}{\partial x}\left(\frac{\rho'}{\rho}\right)\right\}=0 \qquad \text{(continuity)} \qquad (8)$$

$$\left\{\frac{\partial}{\partial t}+u\frac{\partial}{\partial x}\right\}\left(\frac{h'}{h}\right)=0 \qquad \text{(energy)} \qquad (9)$$

$$\frac{h'}{h}=\frac{p'}{p}-\gamma\frac{\rho'}{\rho} \qquad (10)$$

We shall investigate the stability of small periodic disturbances introduced onto the steady state flow, and for convenience the complex variable notation is used. Thus, let

$$\begin{aligned}\frac{u'}{u}&=\mathcal{R}\ell\ f(x)\,e^{\alpha t}\\ \rho'/\rho&=\mathcal{R}\ell\ g(x)\,e^{\alpha t}\\ h'/h&=\mathcal{R}\ell\ s(x)\,e^{\alpha t}\end{aligned} \qquad (11)$$

where

α = complex frequence = $\lambda+i\omega$; λ, ω are real

$f(x)$, $g(x)$, $s(x)$, are in general complex functions of x.

Substituting Eqs. (10) and (11) into Eqs. (7) to (9), the following set of ordinary differential equations is obtained:

$$\alpha f+u\frac{df}{dx}+\frac{\gamma p}{\rho u}\frac{dg}{dx}+\frac{p}{\rho u}\frac{ds}{dx}+\left\{(1-\gamma)g+2f-s\right\}\frac{du}{dx}=0 \qquad (12)$$

$$\alpha g+u\left(\frac{df}{dx}+\frac{dg}{dx}\right)=0 \qquad (13)$$

$$\alpha s+u\frac{ds}{dx}=0 \qquad (14)$$

Since u is a known function of x, Eq. (14) may be integrated, and the set of Eqs. (12) to (14) yield a second order linear differential equation with non constant coefficients.

In principle, it is possible to solve the differential equation in terms of x, α, and three arbitrary constants: C_1, C_2, C_3

$$f = f(x, \alpha, C_1, C_2, C_3)$$
$$g = g(x, \alpha, C_1, C_2, C_3) \qquad (15)$$
$$s = s(x, \alpha, C_3)$$

By applying the boundary conditions at (3) and (5), it is possible to solve for the arbitrary constants, and finally for α in terms of the boundary conditions. Thus $\frac{u'}{u}$, $\frac{\rho'}{\rho}$, $\frac{h'}{h}$ are stable, neutral, or unstable according as $\lambda \lessgtr 0$.

3. Boundary Conditions at Diffusor Inlet, (3)

The detailed treatment of the non-steady flow in the external diffusion regime (i.e., between the shock wave and the diffusor inlet) to determine the boundary conditions at (3) is given in Section D. Only the general results will be utilized.

Since we are dealing with a linear system, it is convenient to represent the boundary conditions at (3) as the density and entropy response of the external diffusion regime that are manifested at (3) due to a periodic velocity input at (3) of arbitrary frequency, ω. That is,

$$(u'/u)_3 = f(x_3, \omega)\, e^{i\omega t}$$
$$(\rho'/\rho)_3 = g(x_3, \omega)\, e^{i\omega t}$$
$$(h'/h)_3 = s(x_3, \omega)\, e^{i\omega t}$$

where $\mathcal{F}$, $\mathcal{G}$, and $\mathcal{S}$ are in general complex numbers since the above flow parameters may differ both in amplitude and phase during the oscillation.

Now define the following ratios,

$$G_3 = (p'/p)_3/(u'/u)_3 = |G_3|\, e^{i\varphi}$$
$$I_3 = (h'/h)_3/(u'/u)_3 = |I_3|\, e^{i\psi} \qquad (16)$$

and since the system is linear, these ratios remain invariant irrespective of the amplitude of $\frac{u'}{u}$.

The amplitude $|G_3|$, $|I_3|$ and the phase shifts φ and ψ are functions of the steady state flow conditions in the external regime (2) to (3), and of the input frequency.

Tsien in Ref. 5 refers to such ratios (G and I) as transfer functions corresponding to the practice of servo-mechanism analysis. He further suggests using the notion of transfer functions for the various components of a complicated oscillatory system, so that the dynamic performance of each may be obtained either experimentally or via calculation, and these synthesized to determine stability. This is, in effect, what is being done in the present analysis, the essential components of the system being: (1) External diffusion regime, (2) Internal duct, (3) Exit nozzle.

Summarizing, the boundary conditions at (3) are given by the transfer functions of Eq. (16).

4. Boundary Conditions at Internal Duct Outlet, (5)

To establish the boundary conditions at (5), one must solve the set of Eqs. (7) to (10) applied to the nozzle regime, and in effect obtain the corresponding transfer functions as discussed in the previous section. This has been done by Tsien in Ref. 5 assuming a linear

steady state axial velocity distribution in the nozzle.

In general, the results are

$$u'/u = f(x,\beta)\, e^{i\omega t}$$

$$\rho'/\rho = g(x,\beta)\, e^{i\omega t}$$

$$h'/h = s(x,\beta)\, e^{i\omega t}$$

where β = reduced frequency = $\omega/\frac{du}{dx}$, and the functions f , g , and s are complex. For small values of β , f , and g may be expanded in a series, viz.

$$f(x,\beta) = f^{(0)}(x) + \beta f^{(1)}(x) + \cdots \beta^n f^{(n)}(x)$$

$$g(x,\beta) = g^{(0)}(x) + \beta g^{(1)}(x) + \cdots \beta^n g^{(n)}(x)$$

For the limiting case $\beta \to 0$, $g^{(0)}(x)$ constant, and $|f^{(1)}(x)| << |f^{(0)}(x)|$ and $|g^{(1)}(x)| << |g^{(0)}(x)|$ but the first order solutions may have a small imaginary component. Neglecting these terms and substituting $f^{(0)}(x)$ and $g^{(0)}(x)$ in Eqs. (12) - (14), the following relationship between velocity, density, and entropy are obtained

$$2f = (\gamma-1)g + s$$

or

$$2\frac{u'}{u} = (\gamma-1)\rho'/\rho + h'/h \qquad (17)$$

but since

$$\frac{a'}{a} = \frac{1}{2}\left[(\gamma-1)\frac{\rho'}{\rho} + \frac{h'}{h}\right]$$

then Eq. (17) yields $\frac{u'}{u} - \frac{a'}{a} = M' = 0$, and therefore the Mach number in the nozzle remains constant during non-steady flow, and the latter may be considered as quasi-stationary.

To get some idea as to the magnitude of β , to check the above

simplified results, the following were estimated:

$$\beta = \omega \Big/ \frac{du}{dx} = \frac{\omega (x^* - x_5)}{(u^* - u_5)}$$

$\omega \doteq 900$ cps $= 5600$ rad/sec. (from experimental data of Section II)

$(x^* - x_5) = 1/4$ in.

$(u^* - u_5) \doteq 1000$ ft./sec.

$\therefore \beta \doteq 0.12$

The calculations for the determination of f and g have been carried out in Ref. 8 and the results are plotted in Ref. 7. A check with these results for the above magnitude of β indicate that the imaginary component is not significant.

Hence, the boundary conditions are given by Eq. (17) applied at (5), viz.

$$2\left(\frac{u'}{u}\right)_5 = (\gamma - 1)\left(p'/p\right)_5 + \left(\frac{h'}{h}\right)_5 \tag{18}$$

5. Development of Stability Criteria

Using the solutions of the non-stationary flow equations given by Eq. (15), and the boundary conditions given by Eqs. (16) and (18), the following set of equations is obtained:

$$\frac{g(x_3, \alpha, c_1, c_2, c_3)}{f(x_3, \alpha, c_1, c_2, c_3)} = G_3$$

$$\frac{s(x_3, \alpha, c_3)}{f(x_3, \alpha, c_1, c_2, c_3)} = I_3 \tag{19}$$

$$2f(x_5, \alpha, c_1, c_2, c_3) = (\gamma - 1) g(x_5, \alpha, c_1, c_2, c_3) + s(x_5, \alpha, c_3)$$

In principle the above set of transcendental equations may be solved in terms of G_3 and I_3. Since for a given diffusor, G_3 and I_3 are a function only of M_1 and M_3, then the magnitude of α and the consequent stability are thereby only a function of M_1 and M_3 (or mass flow).

Now, the above treatment is completely general. However, the functions f and g are extremely difficult to obtain due to the varying cross sectional area (or $u(x)$) which severely complicates Eqs. (12) - (14); and either series expansions or numerical methods possibly must be utilized.

Since the primary objective of the present analysis is the interpretation of the instability rather than a detailed check with experiment for a particular geometric shape, it appeared advisable to select for analysis the diffusor D_5 which has a constant cross section area and is thereby amenable to a relatively simple analysis. This diffusor exhibits essentially the same behavior as regards transition to unstable flow as do the configurations with internal diffusion. In the light of the experimental results, it is felt that the effect of the amount of internal diffusion is in the nature of an aggravating effect rather than the fundamental cause of instability.

C. Development of Stability Criteria for Case of No Internal Diffusion

Regime (3) to (5) has a constant steady state velocity of magnitude $u = u_3 = u_4 = u_5$. Thus, the set of partial differential equations, Eqs. (7) - (9), describing the non-steady flow in the duct become, since $\frac{du}{dx} = 0$:

$$\frac{\partial}{\partial t}\left(\frac{u'}{u}\right) + u\frac{\partial}{\partial x}\left(\frac{u'}{u}\right) + \frac{p}{\rho u}\frac{\partial}{\partial x}\left(\frac{p'}{p}\right) = 0$$

$$\frac{\partial}{\partial t}\left(\frac{\rho'}{\rho}\right) + u\frac{\partial}{\partial x}\left(\frac{\rho'}{\rho}\right) + u\frac{\partial}{\partial x}\left(\frac{u'}{u}\right) = 0 \qquad (20)$$

$$\left(\frac{\partial}{\partial t} + u\frac{\partial}{\partial x}\right)\left(\frac{h'}{h}\right) = 0$$

Also,

$$\frac{a'}{a} = \frac{1}{2}\left(\frac{p'}{p} - \frac{\rho'}{\rho}\right) \qquad (21)$$

Following the technique suggested by Burgers in Ref. 4, Eq. (20) may be transformed to the following characteristic form by eliminating p, ρ, $\frac{p'}{p}$, and $\frac{\rho'}{\rho}$ in terms of a, $\frac{a'}{a}$, and $\frac{h'}{h}$. The solutions may then be obtained practically by inspection.

$$\left\{\frac{\partial}{\partial t} + (u+a)\frac{\partial}{\partial x}\right\}\left(\frac{a'}{a} + \frac{\gamma-1}{2}M\frac{u'}{u} - \frac{1}{2\gamma}\frac{h'}{h}\right) = 0$$

$$\left\{\frac{\partial}{\partial t} + (u-a)\frac{\partial}{\partial x}\right\}\left(\frac{a'}{a} - \frac{\gamma-1}{2}M\frac{u'}{u} - \frac{1}{2\gamma}\frac{h'}{h}\right) = 0 \qquad (22)$$

$$\left(\frac{\partial}{\partial t} + u\frac{\partial}{\partial x}\right)\frac{h'}{h} = 0$$

Also,

$$\frac{p'}{p} = \frac{2\gamma}{\gamma-1}\left(\frac{a'}{a}\right) - \frac{1}{\gamma-1}\left(\frac{h'}{h}\right)$$

$$\frac{\rho'}{\rho} = \frac{2}{\gamma-1}\left(\frac{a'}{a}\right) - \frac{1}{\gamma-1}\left(\frac{h'}{h}\right) \qquad (23)$$

From the nature of the differential operators of Eq. (22), the general form of the solutions are:

$$\frac{a'}{a} + \frac{\gamma-1}{2} M \frac{u'}{u} - \frac{1}{2\gamma}\frac{h'}{h} = F_1[x-(u+a)t] = (\gamma-1) M f_1[x-(u+a)t]$$

$$\frac{a'}{a} - \frac{\gamma-1}{2} M \frac{u'}{u} - \frac{1}{2\gamma}\frac{h'}{h} = F_2[x-(u-a)t] = -(\gamma-1) M f_1[x-(u-a)t] \tag{24}$$

Utilizing Eqs. (23) and (24), the solutions finally become

$$\begin{aligned}
\frac{u'}{u} &= f_1[x-(u+a)t] + f_2[x-(u-a)t] \\
\frac{\rho'}{\rho} &= M\{f_1[x-(u+a)t] - f_2[x-(u-a)t]\} - \frac{1}{\gamma} f_3(x-ut) \\
h'/h &= f_3(x-ut) \\
p'/p &= \gamma M\{f_1[x-(u+a)t] - f_2[x-(u-a)t]\}
\end{aligned} \tag{25}$$

From Eq. (25) one notes that $\frac{u'}{u}$ and $\frac{p'}{p}$ are propagated along the characteristics $\frac{dx}{dt} = u \pm a$ whereas $\frac{h'}{h}$ propagates along the characteristic $\frac{dx}{dt} = u$. That is, the entropy perturbations remain with the fluid particles as they move downstream, whereas velocity and pressure perturbations propagate at the speed of sound up and down stream with respect to the fluid particles. Density perturbations propagate along both sets of characteristics.

Again, as in the previous section since we are interested in periodic disturbances, the general solutions of Eq. (25) become:

$$\begin{aligned}
\frac{u'}{u} &= C_1 e^{\alpha\left(t-\frac{x}{u+a}\right)} + C_2 e^{\alpha\left(t-\frac{x}{u-a}\right)} \\
\rho'/\rho &= MC_1 e^{\alpha\left(t-\frac{x}{u+a}\right)} - MC_2 e^{\alpha\left(t-\frac{x}{u-a}\right)} - \frac{1}{\gamma} C_3 e^{\alpha\left(t-\frac{x}{u}\right)} \\
\frac{h'}{h} &= C_3 e^{\alpha(t-x/u)}
\end{aligned} \tag{26}$$

where as before C_1, C_2, C_3 are the arbitrary complex constants, and

α = complex frequency = $\sigma + i\omega$.

Now applying the boundary conditions at (3), i.e., $x = x_3 = 0$, using Eq. (16):

$$G_3 = \frac{M - M\,C_2/C_1 - \frac{1}{\gamma}\,C_3/C_1}{1 + C_2/C_1}$$

$$I_3 = \frac{C_3/C_1}{1 + C_2/C_1} \tag{27}$$

Applying the boundary conditions at (5), i.e., $x = x_5 = \ell$,

$$e^{-\alpha\left(\frac{\ell}{u+a}\right)} + \frac{C_2}{C_1} e^{-\alpha\left(\frac{\ell}{u-a}\right)} =$$

$$\frac{\gamma-1}{2} M e^{-\alpha\left(\frac{\ell}{u+a}\right)} - \frac{\gamma-1}{2} M \frac{C_2}{C_1} e^{\alpha\left(\frac{\ell}{u-a}\right)} - \frac{\gamma-1}{2\gamma} \frac{C_3}{C_1} e^{-\alpha\frac{\ell}{u}} \tag{28}$$

Solving Eq. (27) for $\frac{C_2}{C_1}$ and $\frac{C_3}{C_1}$ and substituting in Eq. (28), we finally obtain as the governing stability relationship

$$e^{\alpha\tau_1} - \frac{\frac{1}{\gamma} M\, I_3\, e^{-\alpha\tau_2}}{\left(M - G_3 - \frac{1}{\gamma} I_3\right)\left(1 + \frac{\gamma-1}{2} M\right)} = -\left(\frac{1 - \frac{\gamma-1}{2} M}{1 + \frac{\gamma-1}{2} M}\right)\left[\frac{M + G_3 + \frac{1}{\gamma} I_3}{M - G_3 - \frac{1}{\gamma} I_3}\right]$$

$$\text{where} \quad \tau_1 = \frac{2a\ell}{a^2 - u^2} = \frac{2\ell}{a(1-M^2)} \doteq 2\frac{\ell}{a}, \text{ for } M \ll 1 \tag{29}$$

$$\tau_2 = \frac{a\ell}{u(a+u)} = \frac{\ell}{aM(1+M)} \doteq \frac{\ell}{u}$$

τ_1 is a characteristic time of the internal duct and represents the time for propagation of an isentropic wave such as $\frac{\rho'}{\rho}$ or $\frac{u'}{u}$ to travel from the inlet to the nozzle end and back. τ_2 is another characteristic time and represents the time for an entropy wave to traverse the tube.

Equation (29) is a fairly complicated transcendental equation to

solve for α because of the term involving $e^{-\alpha \tau_2}$. However, it can be shown that this term is small compared to the other terms (Cf. Appendix I). Hence, Eq. (29) becomes:

$$e^{\alpha \tau_1} = -\left(\frac{1-\frac{\gamma-1}{2}M}{1+\frac{\gamma-1}{2}M}\right)\left[\frac{M+G_3+\frac{1}{\gamma}I_3}{M-G_3-\frac{1}{\gamma}I_3}\right]$$

$$\text{or} \quad e^{\alpha \tau_1} = -\left(\frac{1-\frac{\gamma-1}{2}M}{1+\frac{\gamma-1}{2}M}\right)\left[\frac{\left(\frac{u'}{u}\right)_3 M+\left\{\left(\frac{p'}{p}\right)_3+\frac{1}{\gamma}\left(\frac{h'}{h}\right)_3\right\}}{\left(\frac{u'}{u}\right)_3 M-\left\{\left(\frac{p'}{p}\right)_3+\frac{1}{\gamma}\left(\frac{h'}{h}\right)_3\right\}}\right] \tag{30}$$

$$\text{or} \quad e^{\alpha \tau_1} = -\left(\frac{1-\frac{\gamma-1}{2}M}{1+\frac{\gamma-1}{2}M}\right)\left[\frac{\left(\frac{u'}{u}\right)_3 M+\frac{1}{\gamma}\left(\frac{p'}{p}\right)_3}{\left(\frac{u'}{u}\right)_3 M-\frac{1}{\gamma}\left(\frac{p'}{p}\right)_3}\right]$$

The absolute value of the term in the square brackets is the ratio of the amplitude of the reflected and impinging waves at the inlet, (3). The term, $-\left(\frac{1-\frac{\gamma-1}{2}M}{1+\frac{\gamma-1}{2}M}\right)$, is the ratio of the amplitudes of the reflected and impinging waves at the nozzle.

Thus, consider a pulse originating in the tube and propagating upstream. It is reflected at the inlet, propagates down stream and is reflected from the nozzle. Thus $|e^{\alpha \tau_1}|$ is the ratio of the pulse amplitude after these two reflections, and the cycle keeps repeating itself in time. If $|e^{\alpha \tau_1}| > 1$, then after each double reflection the amplitude is magnified; and consequently, instability can exist. For $|e^{\alpha \tau_1}| < 1$, the amplitudes after each double reflection are reduced, and the system is stable.

It is interesting to apply this criterion to the simple organ pipe. Now $u = \frac{h'}{h} = 0$, so the above equations become:

$$e^{\alpha \tau_1} = -\left[\frac{\left(\frac{u'}{a}\right)_3 + \frac{1}{\gamma}\left(\frac{p'}{p}\right)_3}{\left(\frac{u'}{a}\right)_3 - \frac{1}{\gamma}\left(\frac{p'}{p}\right)_3}\right]$$

Now using Lagrange's assumption of the open end of the organ pipe being a loop, then $\frac{p'}{p} = 0$.

$$e^{\alpha \tau_1} = -1 \quad , \quad \text{or} \quad e^{\lambda} = 1 \quad , \quad \text{and} \quad e^{i\omega \tau_1} = -1$$

Thus, the system is neutrally stable, since $\lambda = 0$ and $\omega \tau_1 = \pi$ (considering only the fundamental mode). Thus $\omega = \frac{\pi l}{2a}$ rad./sec = $\frac{l}{4a}$ cps.

Rayleigh in Ref. 10 shows that due to escape of energy from the organ pipe mouth $(p'/p)/(u'/a) < 0$, and thus $\lambda < 0$, and the initial oscillations decrease with time.

D. Investigation of Inlet Boundary Conditions

1. Introduction

As indicated in Section B, page 24, the boundary conditions at (3) are given in terms of the transfer functions G_3 and I_3; and these are obtained by solving the non-steady equations of motion in the external diffusion regime.

In formulating a theoretical model of the flow phenomena in the external diffusion region, (2) to (3), it is first necessary to investigate the details of the steady flow conditions just preceding instability, and to then observe the nature of the subsequent superposed linear wave propagations emanating from the inlet and reflected from the shock wave.

Regarding the steady flow, and utilizing the information gleaned

from the schlieren photographs of Figs. 14-17, a qualitative picture of the streamlines as well as the flow details in the vicinity of the lip may be estimated. Figure 20 illustrates the flow characteristics in the vicinity of the inlet lip for stable flow just preceding instability. The stagnation point for the streamline that separates the internal and external flows occurs slightly within the inlet at b. There is a rapid expansion around the lip at d where speeds in excess of sonic are attained, and due to the overexpansion, an oblique shock wave occurs at f. It is possible that a separated region exists just forward of b which reattaches on the external surface as the flow expands around the lip due to the favorable pressure gradient. Since the schlieren photograph of Fig. 14a shows the oblique shock wave origin as very close to the lip, one would estimate the separated zone to be relatively small. Also, it does not appear that the vorticity created at b should propagate into the duct, since the flow forward of b is predominantly out of the inlet. In addition the velocity profiles at the diffusor exit give very little evidence of any significant viscous separation at the duct walls. There is the possibility, however, that just prior to the instability the separation region increases sufficiently to help promote breakdown of the steady state flow. Unfortunately, since the details of the inlet flow could not be directly measured, the above argument is primarily conjecture.

Consequently, in view of the absence of any clear cut evidence of significant lip viscous effects, it appears more fruitful at this time to consider the flow as inviscid. Thus, the objective is to ascertain whether an intrinsic instability can exist independently in whole or in part from viscous effects. If such a tendency can be established, it is then possible that even slight viscous separation effects may be

amplified so as to further aggravate the promotion of instability.

The detached shock wave in the region o - e is only slightly curved (Cf. Figs. 16 and 17) so that for simplicity of analysis it will be assumed as normal to the free stream flow.

As regards the nature of the non-steady flow, Fig. 20 also illustrates wave fronts emanating from the inlet due to a pulse. The wave motion is superposed on the existing steady state flow. The wave fronts which are planar at the inlet begin to spread out, and if there were no shock wave present, they would eventually become spherical. In the region oef, the wave fronts suffer slight distortions since they propagate at the speed of sound relative to the steady state flow. However, in view of the close proximity of the shock wave to the inlet, it appears reasonable to assume that the wave fronts remain fairly planar in region oec. Since the sound waves cannot propagate through the shock wave because of supersonic speeds upstream of the latter, the wave fronts are reflected. Again, since the shock wave is practically normal in the vicinity struck by the upstream moving waves, the reflections should also be essentially planar. Actually not all of the energy contained in the wave front gets reflected from the shock wave, since some propagates outward through eb. Consequently, there is some energy dissipation analogous to that described by Rayleigh (Ref. 10) for the organ pipe resonator. However, this is assumed to be small compared to the wave motion energy that remains within oec. Consequently, we postulate that planar waves issuing from the duct and reflected from the normal shock remain planar, and that all wave motion is restricted to the region oec. A sketch of the postulated theoretical model is shown in Fig. 20.

The above assumptions are necessary in order to make the subsequent analyses somewhat tractable. The exact treatment of the three dimensional linearized non-steady flow in the detached shock wave regime is extremely difficult by nature of the three dimensional aspect of the problem and the complex boundary conditions associated with the curved shock wave and inlet geometry. Consequently, further simplifications such as the assumption of quasi-one dimensional flow within the stream tube bc entering the inlet will be made.

It is felt that the postulated model developed above should preserve the essentials of the phenomena in sufficient degree to enable a first approximation of instability possibilities.

2. General Treatment of Flow within External Diffusion Regime

a. Boundary Conditions at the Shock Wave

From the results obtained in Ref. 9, one can show that the non-steady, slightly curved shock wave such as occurs in the region, oe, of Fig. 20 can be replaced by a normal shock without causing any significant change.

In Ref. 4, Burgers treats the case of planar sound waves striking a normal shock wave, and derives the resulting reflections. Consider the following diagram showing the shock wave in motion with a velocity, ξ, relative to the free stream flow. Since the shock wave is practically a discontinuity, it is possible to neglect time derivatives of any of the parameters within the shock wave, and so the Rankine-Hugoniot relations developed for a stationary shock wave apply. The shock wave is made stationary by superposing a flow of velocity, ξ, moving upstream,

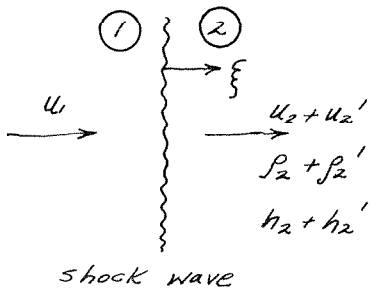

$( )'$ = perturbations due to shock wave motion

and the momentum, continuity, energy, and equation of state relations are applied. Thus

$$
\begin{aligned}
&p_1 + \rho_1(u_1 - \xi)^2 = (p_2 + p_2') + (\rho_2 + \rho_2')(u_2 - \xi + u_2')^2 \\
&\rho_1(u_1 - \xi) = (\rho_2 + \rho_2')(u_2 - \xi + u_2') \\
&c_p T_1 + \tfrac{1}{2}(u_1 - \xi)^2 = c_p(T_2 + T_2') + \tfrac{1}{2}(u_2 - \xi + u_2')^2 \\
&p + p' = R(\rho + \rho')(T + T')
\end{aligned}
\tag{31}
$$

Now assuming that $\frac{\xi}{u_2}$, $\frac{u_2'}{u_2}$, $\frac{p_2'}{p_2}$, $\frac{\rho_2'}{\rho_2}$, $\frac{T_2'}{T_2}$, are all $<< 1$, and retaining only first order terms of these parameters, the above set of equations may be solved in terms of the shock velocity, ξ. Thus, we obtain

$$
\begin{aligned}
&\frac{u_2'}{u_2} = \frac{2}{\gamma+1}\left(1 + \frac{1}{M_1^2}\right)\xi/u_2 \\
&\rho_2'/\rho_2 = -\frac{4}{\gamma+1}\,\frac{1}{M_1^2}\,\xi/u_2 \\
&p_2'/p_2 = -\frac{4}{\gamma+1}\left(\frac{1 + \frac{\gamma-1}{2}M_1^2}{\gamma M_1^2 - \frac{\gamma-1}{2}}\right) \\
&\frac{h_2'}{h_2} = \frac{p_2'}{p_2} - \gamma\frac{\rho_2'}{\rho_2} = -\frac{4\gamma}{\gamma+1}\left\{\frac{(\gamma-1)M_1^2\left(\frac{M_1^2}{2} - 1\right) + \frac{\gamma-1}{2}}{\left(\gamma M_1^2 - \frac{\gamma-1}{2}\right)M_1^2}\right\}
\end{aligned}
\tag{32}
$$

These quantities are plotted in Fig. 21 as function of M_1. It is seen that there is a resulting entropy perturbation, $\frac{h'}{h}$, which is negligible for free stream Mach numbers close to one, but increases with increasing M_1. Another significant result to note is that $\rho'/\rho \to 0$ as $M_1 \to \infty$.

Now let us consider the nature of the reflected waves. Consider

an isentropic compression sound wave $\left(\frac{h'}{h}=0\right)$ moving upstream. Thus both $\frac{\rho'}{\rho}$ and $\frac{h'}{h}$ are >0, and $\frac{u'}{u}<0$. The shock wave, upon being struck by a sound wave, instantaneously moves forward and achieves a velocity, ξ, to match the $\frac{u'}{u}$ boundary condition. As a consequence, an entropy perturbation, $\frac{h'}{h}$, developes, and the resulting pressure density relation is modified via $\frac{p'}{p}=\gamma\frac{\rho'}{\rho}+\frac{h'}{h}$. From the nature of the one dimensional wave propagation as given in Eq. (25), it is seen that the reflected pressure wave propagates at the speed of sound whereas the entropy wave propagates at only the speed, u, of the local flow.

By way of summary, when an isentropic wave strikes the shock wave, both isentropic and entropy waves are reflected traveling at speeds $u+a$, and u respectively. A compression wave reflects as a rarefaction wave similar to the phenomena at the open end of an organ pipe. The boundary conditions at the shock wave as a function of M_1 are given in Eq. (32), and plotted in Fig. 21.

b. Non-Steady Linearized Equations of Motion Applicable to External Diffusion Regime

Considering axial symmetry, the linearized momentum, continuity, and energy equations are:

$$\frac{u}{r}\frac{\partial}{\partial t}\left(\frac{u'}{u}\right)+\frac{\partial}{\partial x}\left\{(\rho u^2)\left(2\frac{u'}{u}+\frac{\rho'}{\rho}\right)\right\}+\frac{1}{r}\frac{\partial}{\partial r}\left\{(r\rho u v)\left(\frac{\rho'}{\rho}+\frac{u'}{u}+\frac{v'}{v}\right)\right\}=-p\frac{\partial}{\partial x}\left(\frac{p'}{p}\right)-\left(\frac{p'}{p}\right)\frac{\partial p}{\partial x} \qquad (33)$$

$$\frac{v}{r}\frac{\partial}{\partial t}\left(\frac{v'}{v}\right)+\frac{\partial}{\partial x}\left\{(\rho u v)\left(\frac{\rho'}{\rho}+\frac{u'}{u}+\frac{v'}{v}\right)\right\}+\frac{1}{r}\frac{\partial}{\partial r}\left\{(r\rho v^2)\left(\frac{\rho'}{\rho}+2\frac{v'}{v}\right)\right\}=-p\frac{\partial}{\partial r}\left(\frac{p'}{p}\right)-\left(\frac{p'}{p}\right)\frac{\partial p}{\partial r}$$

$$\frac{\rho}{r}\frac{\partial}{\partial t}\left(\frac{\rho'}{\rho}\right) + \frac{\partial}{\partial x}\left\{(\rho u)\left(\frac{\rho'}{\rho} + \frac{u'}{u}\right)\right\} + \frac{1}{r}\frac{\partial}{\partial r}\left\{(r\rho v)\left(\frac{\rho'}{\rho} + \frac{v'}{v}\right)\right\} = 0$$

$$\left(\frac{\partial}{\partial t} + u\frac{\partial}{\partial x} + v\frac{\partial}{\partial r}\right)\left(\frac{h'}{h}\right) = 0$$

$$\frac{h'}{h} = \frac{p'}{p} - \gamma\rho'/\rho$$

As noted from the energy equation, the entropy perturbations are propagated along the steady state streamlines. Thus referring to Fig. 20, it is seen that when a planar wave emanating from the inlet strikes the shock wave a portion of the resulting generated entropy wave propagates into the stream tube corresponding to that portion of the shock wave ob intercepted by the bounding stream lines of the internal stream tube. The entropy generated by the remainder of the shock wave (be) spills out around the diffusor internal stream tube.

The set of Eqs. (33) are extremely difficult to solve. Consequently, at this point the following quasi-one dimensional assumptions are made: ρ, u, p, u'/u, ρ'/ρ, p'/p within the bounding regions, oec, affected by the wave motion are independent of r, and are functions of x, t only. $\frac{v'}{v}$ is still retained as a function of x, r, t, but within the internal stream tube, v is considered small. Thus, in effect the vertical momentum equation is neglected. The latter is a reasonable assumption since $v \doteq 0$ at b, and $v = 0$ at c.

It is convenient to integrate Eq. (33) with respect to r from $r = 0$ to $r = \mathcal{R}$, where $\mathcal{R}$ denotes the ordinate to the steady state streamline (Cf. Fig. 20).

Using the above assumptions, the integration within the stream tube may most easily be carried out by applying the axial momentum and continuity equations to the cross hatched area. Also, the inlet station (3) has now been moved back slightly to the stagnation point c. Thus,

the equations become:

$$\rho A \frac{\partial \bar{u}}{\partial t} + \frac{\partial(\rho \bar{u}^2 A)}{\partial x} + \rho \bar{u}\,(V\cos m - \bar{u}\sin m)\,2\pi R\,dz = -\frac{\partial p}{\partial x}$$

$$A\frac{\partial \rho}{\partial t} + \frac{\partial(\rho \bar{u} A)}{\partial x} + \rho\,(V\cos m - \bar{u}\sin m)\,2\pi R\,dz = 0 \qquad (34)$$

$$\left(\frac{\partial}{\partial t} + \bar{u}\frac{\partial}{\partial x}\right) H = 0$$

Now

$$\rho = \rho + \rho' \qquad V = v + v'$$

$$p = p + p' \qquad A = \pi R^2$$

$$\bar{u} = u + u'$$

And using the steady state relations

$$d(\rho u A) = 0$$

$$u\,du = -\frac{1}{\rho}\,dp$$

$$v\cos m - u\sin m = 0$$

Equations (34), in linearized form, become:

$$\frac{\partial}{\partial t}\left(\frac{u'}{u}\right) + \frac{\partial}{\partial x}\left\{u\left(2\frac{u'}{u} + \frac{\rho'}{\rho}\right)\right\} + u\left(\frac{v'}{v} - \frac{u'}{u}\right)2\,\frac{dR}{R} = -\frac{1}{\rho u}\left\{p\frac{\partial}{\partial x}\left(\frac{p'}{p}\right) - \rho u\left(\frac{p'}{p}\right)\frac{du}{dx}\right\}$$

$$\bar{u}'\frac{\partial}{\partial t}\left(\frac{\rho'}{\rho}\right) + \frac{\partial}{\partial x}\left\{\frac{p'}{p} + \frac{u'}{u}\right\} + \left(\frac{v'}{v} - \frac{u'}{u}\right)2\,\frac{dR}{R} = 0 \qquad (35)$$

$$\left(\frac{\partial}{\partial t} + u\frac{\partial}{\partial x}\right)\frac{h'}{h} = 0$$

The term $\pi R^2 \rho u\left(\frac{v'}{v} - \frac{u'}{u}\right)2\frac{dR}{R} = \rho(v'\cos m - u'\sin m)\,2\pi R\,dz$

represents the mass flux through the control surface.

Equation (35) is identical to Eqs. (7) - (9) describing the quasi-one dimensional flow within the duct with the exception of the

boundary mass flux term.

To solve the set of Eqs. (35), for an arbitrary oscillation frequency, ω, we set

$$\frac{u'}{u} = f(x)\, e^{i\omega t} \quad , \quad \frac{h'}{h} = s(x)\, e^{i\omega t}$$
$$\frac{\rho'}{\rho} = g(x)\, e^{i\omega t} \quad , \quad \frac{v'}{v} = q(x)\, e^{i\omega t} \tag{36}$$

which yields a set of ordinary differential equations in $f, g, s,$ and q in terms of x, ω, t. Solving this set and substituting the boundary conditions at the shock wave*, it is finally possible to obtain $(u'/u)_3$, $(\rho'/\rho)_3$, and $(h'/h)_3$ as functions of ω.

The above set of ordinary differential equations are more complicated than the corresponding ones describing the nozzle flow, i.e., Eqs. (7) to (10), due to the presence of the mass flux term. However, it can be shown that the time dependent terms are negligible due to the large axial velocity gradient, and thus quasi-steady results can be used. The proof for this will be given in the following section.

3. Use of Quasi-Steady Flow in the External Diffusion Regime

In order to establish the magnitude of the time dependent terms of Eq. (35), the mass flux term, $\left(\frac{v'}{v} - \frac{u'}{u}\right)$, was neglected in order to make the problem tractable. The normal shock boundary conditions of Eq. (32) were retained. Thus, these equations and boundary conditions describe the non-steady flow phenomena for the external diffusion regime as

---

* Must now consider the shock wave as slightly curved in order to obtain v'/v at the shock wave.

completely confined within the internal flow stream tube. It is felt that the neglect of the mass flux term should not have any significant effect on the comparative magnitude of the steady and non-steady terms of Eq. (35).

Substituting Eq. (36) into the above described modified Eq. (35), the set of ordinary differential equations, Eqs. (12) - (14), is obtained where now $\alpha = \omega$ (real frequency). Now, replace the independent variable x by u via $\frac{d}{dx} = \frac{1}{u_2}\frac{du}{dx}\frac{d}{dy}$, where $y = \frac{u}{u_2}$. Thus, Eqs. (12) - (14) become:

$$
\begin{aligned}
&i\beta f + y\frac{df}{dy} + \frac{a^2}{uu_2}\frac{dg}{dy} + \frac{a^2}{\gamma u u_2}\frac{ds}{dy} + (1-\delta)g + 2f - s = 0 \\
&i\beta g + y\left(\frac{df}{dy} + \frac{dg}{dy}\right) = 0 \\
&i\beta s + y\frac{ds}{dy} = 0 \\
&\text{where} \quad \beta = \omega \Big/ \left(\frac{du}{dx}\right) = \text{reduced frequency}
\end{aligned}
\tag{37}
$$

Now, we assume $\frac{du}{dx}$ = constant; thus β = constant, and the last equation of Eq. (37) can be integrated, viz.

$$\log s = -i\beta \log y + C$$

Applying the boundary conditions of Eq. (32), $s = s_2$ at $y = 1$

$$s = s_2 y^{-i\beta} = s_2 e^{-i\beta \log y} \tag{38}$$

where $\frac{h'}{h} = s_2 \frac{\xi}{u_2}$, and $\xi = \xi_0 e^{i\omega t}$

Substituting Eq. (38) into (37), we obtain:

$$
\begin{aligned}
&y\frac{df}{dy} + \frac{a^2}{uu_2}\frac{dg}{dy} + (1-\delta)g + (2+i\beta)f = s_2 e^{-i\beta\log y}\left[1 + \frac{i\beta}{\gamma M^2}\right] \\
&y\frac{df}{dy} + y\frac{dg}{dy} + i\beta g = 0
\end{aligned}
\tag{39}
$$

where $\frac{a^2}{u u_2} = \frac{(1+\frac{\gamma-1}{2}M_2^2)}{\gamma M_2^2} - \frac{\gamma-1}{2}\gamma \doteq \frac{1}{\gamma M_2^2}$

Now f and g are in general complex. Thus the boundary conditions at $y=1$ (the shock wave) are:

$Re\, f = f_2$ where $\frac{u_2'}{u_2} = \frac{\xi}{u_2} f_2$

$Im\, f = 0$

$Re\, g = g_2$ where $\rho_2'/\rho_2 = \frac{\xi}{u_2} g_2$

$Im\, g = 0$ and $\xi = \xi e^{i\omega t}$

and f_2, g_2 are obtained from Eq. (32).

We now seek solutions to Eq. (34) with the above shock wave boundary conditions. Eqs. (39) are identical to those obtained for the non-steady nozzle flow (Ref. 5), and combining the two equations yields a non-homogeneous hypergeometric differential equation. For $\beta \to 0$, the terms containing $i\beta$ can be neglected, and thus the resulting terms f and g are real. This is equivalent to neglecting the terms involving the time derivatives; $\frac{\partial}{\partial t}\left(\frac{u'}{u}\right)$, $\frac{\partial}{\partial t}\left(\frac{\rho'}{\rho}\right)$, and $\frac{\partial}{\partial t}\left(\frac{h'}{h}\right)$, in Eq. (35). Thus, it is possible to use only the steady state differential equations considering the phenomena as quasi-stationary. Hence, the transfer functions are real and no phase shifts are involved.

Also, $\beta = \omega \Big/ \left(\frac{du}{dx}\right) = \frac{2\pi A}{\lambda_w \left(\frac{du}{dx}\right)} \doteq \frac{2\pi (x_3 - x_2)}{\lambda_w (M_3 - M_2)}$

where λ_w = wave length. Thus, $\beta \to 0$ indicates that for given steady velocity conditions (M_2, M_3) existing in the external diffusion region, the ratio of the length of this region to the wave length is small.

We now evaluate the order of magnitude of β using the experimental data of Section II. For diffusor D_5, $f = 870$ cps,

$a \doteq 1000$ ft/sec., $(x_3 - x_2) = 0.145$ in. at $M_1 = 2.0$, $M_2 = 0.578$, $M_3 = 0.1$

$\lambda_w = a/f = 1.15$ ft.

$\therefore \beta = -0.14$

The set of Eqs. (39) were solved using the Reeves Analog Computer of the Jet Propulsion Laboratory for the shock wave boundary conditions given in Eq. (32) and for the following conditions:

$$M_1 = 1.5,\ 2.0,\ 3.0,\ 4.0$$
$$\beta = 0,\ -0.1,\ -0.2,\ -0.3$$

The results corresponding to $M_1 = 3.0$ are shown in Fig. 23. As can be seen there is a small imaginary component for $\beta = -0.14$ in both f and g. However, the resulting phase shift in $G = g/f$ for the region of interest, $y > 0.1$, is small. The phase shift in **s** may be obtained from Eq. (38), and for $y > 0.1$ is less than 18°.

Graphical constructions to solve the stability equations, Eqs. (30), were made to determine the magnitude of the phase shifts in the transfer functions, G and I, that would be significant in affecting the results as compared to the case of no phase or time lags. It was found that phase lags below about 20° showed no significent effect on stability.

Hence, one can conclude that for the magnitudes of $|\beta| < 0.2$ the flow phenomena in the external regime may be considered as quasi-steady.

4. Solution of the Simplified Equations of Motion, and Determination of Inlet Boundary Conditions

Considering the motion as quasi-steady, the terms of Eq. (35)

involving time derivatives are neglected and the resulting equations are given below:

$$
\begin{aligned}
&u\frac{d}{dx}\left(\frac{u'}{u}\right)+\frac{a^2}{u}\frac{d}{dx}\left(\frac{\rho'}{\rho}\right)+\left[2\frac{u'}{u}+(1-\gamma)\frac{\rho'}{\rho}-\frac{h'}{h}\right]\frac{du}{dx}=0\\
&\frac{d}{dx}\left(\frac{\rho'}{\rho}\right)+\frac{d}{dx}\left(\frac{u'}{u}\right)+\left(\frac{v'}{v}-\frac{u'}{u}\right)\frac{d}{dx}\left[\log\left(R/R_2\right)^2\right]=0\\
&\frac{d}{dx}\left(\frac{h'}{h}\right)=0
\end{aligned}
\tag{40}
$$

Since the velocity wave fronts emanating from the duct inlet and reflected from the shock wave are almost planar in the region of the internal stream tube,* we can conclude that $\frac{v'}{v} << \frac{u'}{u}$ on the control surface (which is the bounding surface of the internal stream tube).

Furthermore, making the transformation: $\frac{d}{dx}=\frac{1}{u_2}\frac{du}{dx}\frac{d}{dy}$ where $y=\frac{u}{u_2}$ and letting $\left(\frac{\rho}{R_2}\right)^2=\frac{A}{A_2}$, Eqs. (40) in terms of the amplitudes of $\frac{u'}{u}$, $\frac{\rho'}{\rho}$, and $\frac{h'}{h}$ (Cf. Eq. (36)) finally become:

$$
\begin{aligned}
&y\frac{df}{dy}+\left(\frac{a}{a_2}\right)^2\frac{1}{M_2^2 y}\frac{dg}{dy}+2f+(1-\gamma)g-S=0\\
&\frac{df}{dy}+\frac{dg}{dy}-f\frac{d}{dy}\left(\log A/A_2\right)=0
\end{aligned}
\tag{41}
$$

where,

$$
\begin{aligned}
&y\left(\frac{a_2}{a}\right)^2=\frac{M}{M_2}\left(\frac{a_2}{a}\right)=\frac{M}{M_2}\sqrt{\frac{1+\frac{\gamma-1}{2}M^2}{1+\frac{\gamma-1}{2}M_2^2}}\\
&A/A_e=\frac{M_2}{M}\left[\frac{1+\frac{\gamma-1}{2}M^2}{1+\frac{\gamma-1}{2}M_2^2}\right]^{\frac{1}{2}\left(\frac{\gamma+1}{\gamma-1}\right)}
\end{aligned}
\tag{42}
$$

Using the relationships of Eq. (42), it was found that Eqs. (41) could most easily be solved by numerical integration using the boundary conditions at the shock wave as given in Eq. (32) and plotted in Fig. 21. The entropy perturbation is now, $S=\left(\frac{A_2}{A_3}\right)S_2$.

The results in terms of ρ'/ρ and u'/u as a function of y

---

* See discussions in introduction of this section.

(which are proportional to g and f respectively) are shown in Fig. 23 for M_1 = 2, 3, and 4. For all values of y and M_1, $\frac{u'}{u} > 0$; and approaches infinity as $y \to 0$. A significant result to note is the behavior of ρ'/ρ. For a given M_1, $\rho'/\rho < 0$ at the shock wave $(y=1)$. However, as y is decreased corresponding to a reduced mass flow into the duct, $\frac{\rho'}{\rho}$ increases, and for sufficiently low y, $\rho'/\rho > 0$. This tendency increases as the free stream Mach number, M_1, increases, and cross over to $\rho'/\rho > 0$ occurs at larger values of y.

As has been shown in the section on stability criteria, a necessary condition for instability to exist is that $\rho'/\rho > 0$. This will be further developed in a subsequent section.

There are two significant causes that make $\rho'/\rho > 0$. First, the diffusion process from the shock wave to the inlet causes the slope, $\frac{d}{dy}\left(\frac{\rho'}{\rho}\right)$, to be negative. Second, as M_1 is increased, ρ'/ρ, although still remaining negative, decreases in absolute magnitude (Cf. Fig. 21).

The pressure perturbation at the inlet is

$$\left(\frac{p'}{p}\right)_3 = \gamma\left(\frac{\rho'}{\rho}\right)_3 + \left(\frac{h'}{h}\right)_3 \qquad \text{where} \quad \left(\frac{h'}{h}\right)_3 = \left(\frac{A_2}{A_3}\right)\left(\frac{h'}{h}\right)_2$$

and since $\frac{A_2}{A_3} = y$, then $\left(\frac{p'}{p}\right)_3 = \gamma\left(\frac{\rho'}{\rho}\right)_3 + y\left(\frac{h'}{h}\right)_2$

E. Application of Stability Criteria

Using the results of the previous section and applying the stability criteria of Eq. (30), we obtain:

$$e^{\alpha \tau_1} = -\left(\frac{1 - \frac{\gamma-1}{2}M}{1 + \frac{\gamma-1}{2}M}\right)\left[\frac{\left(\frac{u'}{u}\right)_3 M + \left\{\left(\frac{\rho'}{\rho}\right)_3 + \frac{1}{\gamma}y\left(\frac{h'}{h}\right)_2\right\}}{\left(\frac{u'}{u}\right)_3 M - \left\{\left(\frac{\rho'}{\rho}\right)_3 + \frac{1}{\gamma}y\left(\frac{h'}{h}\right)_2\right\}}\right]$$

where $\alpha = \lambda + i\omega$

$$\tau_1 = \frac{2l}{a}\frac{1}{(1-M^2)}$$

$\left(\frac{u'}{u}\right)_3$ and $\left(\frac{p'}{p}\right)_3$ as functions of γ and M_1 are obtained from Fig. 23. $\left(\frac{h'}{h}\right)_2$ is obtained from Fig. 21. Instability, $\lambda > 0$, occurs when $|e^{\alpha\tau_1}| > 0$. Since the right hand side is real then a necessary condition for instability is that $\left\{\left(\frac{p'}{p}\right)_3 + \frac{1}{\gamma}\gamma\left(\frac{h'}{h}\right)_2\right\} > 0$. The stability boundary corresponding to $\lambda = 0$, i.e., M vs. M_1, has been determined applying the above results and is shown in Fig. 24.

The corresponding frequency is determined by equating $e^{i\omega\tau_1} = -1$, or $\omega\tau_1 = \pi(2n+1)$, where $n = 0, 1, 2, \ldots$ Thus,

$$\omega = \frac{(2n+1)\pi a}{2l(1-M^2)} \text{ rad./sec.} = (2n+1)\frac{a}{4l(1-M^2)} \text{ cps}$$

which is approximately the natural frequency of an organ pipe.

Referring to Fig. 24, it is noted that the stability boundary has the same trend with M_1 as does the experimental results. Also, the resulting frequency of instability is approximately equal to that of the observed results (Cf. Section II).

F. Summary

1. Stability Criteria

The stability of a system consisting of a diffusor, plenum chamber, and choked exit nozzle is primarily a function of the inlet conditions, and to a lesser degree of the exit nozzle conditions.

A necessary condition for instability to exist is that the ratio of the amplitudes of the reflected and impinging waves at the inlet be greater than one. In terms of the boundary conditions at the diffusor

inlet, this means that the ratio of the pressure and velocity perturbations (transfer function) at the inlet during non steady flow must be positive. For the case where the transfer function is complex, a necessary condition for instability is that its real part be positive.

2. Non-Steady Flow Inlet Conditions

Assuming no significant viscous effects at the inlet lip, and thus postulating inviscid flow in the external diffusion region, it appears possible to obtain a positive transfer function at the inlet regime.

In view of the approximations necessary to solve the non-steady equations of motion in the external diffusion regime, only the orders of magnitudes and trends of the results with inlet mass flow and free stream Mach number are significant.

It is possible to consider the non-steady flow phenomena in the external diffusion regime as quasi-steady because of the close proximity of the detached shock wave and the inlet, as compared to the wave length of the oscillatory flow.

3. Existence of Instability

An instability independent of viscous effects can be predicted which exhibits a stability boundary that has the same trend with mass flow, and free stream Mach number as does the experimental results.

In addition, the resulting frequency at instability corresponds closely to the internal duct acting as an organ pipe which is in agreement with observed results.

The basic causes of the positive transfer function at the inlet

and consequent instability are primarily due to the following:

1. The diffusion process from the detached shock wave to the inlet causes the pressure perturbation at the inlet to increase as the steady state inlet Mach number is decreased.

2. As M_1 is increased the absolute magnitude of the pressure and density perturbations just behind the detached shock wave decreases.

IV. RECOMMENDATIONS

The experimental and theoretical investigations described in Sections II and III were of an exploratory nature, and they served the intended purposes of exhibiting the existence of a possible intrinsic instability and yielding a clue as to its cause.

Consequently, further studies, in the nature of refinements and extensions of the above investigations, should be pursued to help firmly establish the phenomenological model, and in particular to measure the validity of the postulates and assumptions used in the present theoretical investigations.

In addition, future studies should attempt, also, to extend the results of the normal shock diffusors to the Oswatitsch type. In particular, the interaction between boundary layer effects and the normal tendency towards intrinsic instability should be investigated.

Thus, for subsequent investigations of the normal shock type diffusors, the following approaches are suggested:

A. To ascertain the details of the three-dimensional steady flow field just preceding instability, it is suggested that interferometric measurements of the external diffusion regime be made.

Along these line, it may be desirable to restrict the investigation to two-dimensional models both because of the inherently-simple interpretation of the interferograms that exist and because flow details within the diffusor duct can be exhibited.

B. The nature of the wave propagations, particularly in the external diffusion regime, as the mass flow is reduced to the instability point, can be studied by pulsing the exhaust throttle at various

frequencies and observing the subsequent motion by means of interferometric photographs taken at short (known) time intervals.

C. In addition to the above studies, direct measurements of the diffusor inlet transfer function can be made by measurements of instantaneous static pressure and velocity in the vicinity of the inlet. For the pressure measurements, a crystal-type pickup can be used, and an approximate measure of the instantaneous velocity may be measured approximately by a hot-wire anemometer.

It is possible to obtain more refined measurements of the velocity by using the density values obtained from the interferometer investigations in conjunction with the hot-wire measurements.

These inlet transfer function measurements should be made for various steady state mass flows as the latter are reduced to the instability point. This can be done by pulsing the exhaust throttle with a small-amplitude periodic motion at various frequencies below and above the natural frequency of the duct. From the resulting pressure and velocity measurements, it is possible to evaluate the complex transfer function as a function of input frequency.

D. Further analytic studies to determine the effect of internal diffusion on the stability criteria should be pursued.

V. CONCLUSIONS

From experimental investigations of normal shock conical diffusors, it was observed that self-excited oscillations could occur as the mass flow was reduced below its maximum value. Qualitatively, the phenomena are strikingly similar to the instability associated with the inner body (or Oswatitsch) type diffusors. The above experimental results indicate the following:

1. Increasing the free stream Mach number aggravates the instability condition in that larger relative mass flows are required to achieve stable flow. However, no instability could be detected below a free stream Mach number of approximately 1.8.
2. For a given free stream Mach number, instability occurred at increasing relative mass flows as the amount of internal diffusion was increased.
3. Frequencies of the self-excited oscillations were approximately equal to the natural frequency of the internal duct acting as an organ pipe resonator (i.e., one quarter wave length).
4. Modifying the diffusor lip shape or varying the lengths of the plenum chamber did not significantly affect the occurrence of instability.
5. Flow within the diffusor just prior to the onset of instability, as well as that in the neighborhood of the inlet lip, showed no significant viscous separation effects.

From the results of theoretical investigations which were carried out in order to help interpret the above experimental observations, it

is possible to show the existence of an intrinsic instability (i.e., independent of viscous effects) that exhibits the same trend with mass flow and Mach number as does the experimental results. The instability is primarily dependent upon inlet flow conditions. Postulating an inviscid flow, and considering the configuration with no internal diffusion, the following are the significant results.

1. A necessary condition for the existence of instability is that the ratio of the amplitudes of the reflected and impinging waves at the diffusor inlet be greater than one.

   In terms of the boundary conditions at the inlet, this implies that the transfer function (ratio of pressure to velocity perturbations) there is positive.

2. It is possible to obtain a positive value of the inlet transfer function and consequent instability due to the combination of the following effects.

   (a) The normal steady state compression that exists between the shock wave and inlet, causes the density and pressure perturbations to increase as the inlet Mach number (or mass flow) decreases.

   (b) The above compression process in the external diffusor regime is practically isentropic since at the low mass flows, the entropy perturbations caused by the pulsing shock wave are convected along the steady state stream lines which spill over around the inlet. Thus, only a small portion of the generated entropy waves are reflected back into the duct, which

in effect tends to increase the pressure perturbations there.

(c) As the free stream Mach number increases, the density and pressure perturbations just downstream of the pulsing shockwave, that are normally negative, decrease in absolute magnitude.

3. The results of the theoretical investigation indicate a rough check with experiment in that they exhibit both the lower limit in free stream Mach number below which no instability exists ($M \doteq 1.8$), and for Mach numbers above this, instability occurs at increasing mass flows.

Consequently, it appears that the instability associated with normal shock diffusors at supersonic speeds can in part be of an intrinsic nature.

4. Increasing the mass flow through the diffusor has a double effect in eliminating an instability, since it reduces the amount of diffusion in the inlet regime, and also decreases the amount of wave motion energy reflected at the nozzle end (or duct exit).

5. It is possible to determine, at least qualitatively, the effect of the diffusor on the instability of a complete air breathing engine, by replacing the nozzle transfer function by the corresponding one for the combustion chamber (either measured or calculated), and applying the derived stability criteria.

In general one can conclude that the presence of a

diffusor tends to aggravate the possibility of instability of an air breathing engine in the sub-critical flow regime. This occurs since the ratio of the amplitudes of reflected to impinging waves at the diffusor inlet increases as the mass flow decreases.

6. In view of the quasi-one dimensional flow approximations that were necessary in order to solve the non-steady equations of motion in the external diffusion and exit nozzle regimes, the above conclusions are pertinent only to the axial modes of oscillation.

Because of the relatively short length of the external diffusion regime it is to be expected that some errors will result by virtue of neglecting the transverse wave propagations.

For applications of the above results to cases in which the natural frequency of the system is sufficiently high so that the reduced frequency is above,say one-third, it is necessary to consider the transfer functions as complex in applying the stability criteria.

7. Finally, as regard to the more complex instability phenomena associated with the Oswatitsch type diffusors, it seems plausible to consider the tendency towards an intrinsic instability (such as occurs in the normal shock diffusors) as an additional effect that must be combined with viscous separation effects in attempting to explain the phenomena.

REFERENCES

1. Oswatitsch, K.: "Pressure Recovery for Missiles with Reaction Propulsion at High Supersonic Speeds", NACA Translation Tech. Memo No. 1140, (1944).

2. Hartmann, J.: "On the Production of Acoustic Waves by Means of a Velocity Exceeding that of Sound", Philosophical Magazine and Journal of Science (1931), Vol. II, p. 926.

3. Lukasiewicz, J.: "Supersonic Diffusors", Aeronautical Research Council Reports and Memoranda No. 2501, (1952).

4. Burgers, J. M.: "On the Transmission of Sound Waves Through a Shock Wave", Koninklijke Nederlandsche Akadamie Van Wetenschappen, (1946), Vol. XLIX.

5. Tsien, H. S.: "The Transfer Function of Rocket Nozzles", Journal of the American Rocket Society (May, 1952), Vol. 22, No. 3, p. 139.

6. Crocco, L.: "Aspects of Combustion Stability in Liquid Propellant Rocket Motors. Part II: Low Frequency Instability with Bi-Propellants. High Frequency Instability", Journal of the American Rocket Society, (Jan. 1952), Vol. 22, No. 1, p. 7.

7. Crocco, L. and Cheng, S.: "High Frequency Combustion Instability in Rockets with Distributed Combustion", Princeton University Aeronautical Engineering Laboratory, (Sept. 1952).

8. Crocco, L.: "Supercritical Gaseous Discharge with High Frequency Oscillation", Paper Presented at the 8th International Congress of Applied Mathematics and Mechanics, (Aug. 1952).

9. Moore, F. K.: "Unsteady Oblique Interaction of a Shock Wave with a Plane Disturbance", NACA TN 2879, (Jan. 1953).

10. Lord Rayleigh: "The Theory of Sound", Dover Publications, New York, (1945).

11. Ferri, A. and Nucci, L. M.: "Preliminary Investigation of a New Type of Supersonic Inlet", NACA TN 2286, (April, 1951).

12. Prandtl, L.: "Neue Untersuchungen über die Strömende Bewegung der Gasse und Dämffe", Physikalische Zeitschrift, (1907), Vol. 8, pp. 23-32.

13. Puckett, A. E.: "Final Report, Model Supersonic Wind Tunnel Project", Contract NDC rc-36, (Nov., 1943).

14. Meyer, R. E.: "On Waves of Finite Amplitude in Ducts", The Quarterly Journal of Mechanics and Applied Mathematics (Sept., 1952), Vol. V, Part 3, pp. 257-291.

15. Minorsky, N.: "Introduction to Non-Linear Mechanics", Published by J. W. Edwards, Ann Arbor, Michigan, (1947).

APPENDIX I

DERIVATION OF SIMPLIFIED EXPRESSION FOR THE STABILITY CRITERIA

In Eq. (29), transposing the term in involving $e^{-\alpha\tau_2}$, we obtain:

$$e^{\alpha\tau_1} = -\left(\frac{1-\frac{\gamma-1}{2}M}{1+\frac{\gamma-1}{2}M}\right)\left[\frac{M+G_3+\frac{1}{\gamma}I_3\left\{1-\frac{Me^{-\alpha\tau_2}}{1-\frac{\gamma-1}{2}M}\right\}}{M-G_3-\frac{1}{\gamma}I_3}\right]$$

In the neighborhood of instability $\lambda > 0$

Thus, $\left| e^{-\alpha\tau_2} \right| < 1$

and also since we are concerned with small M, then

$$\left(\frac{Me^{-\alpha\tau_2}}{1-\frac{\gamma-1}{2}M}\right) << 1$$

and Eq. (30) is obtained.

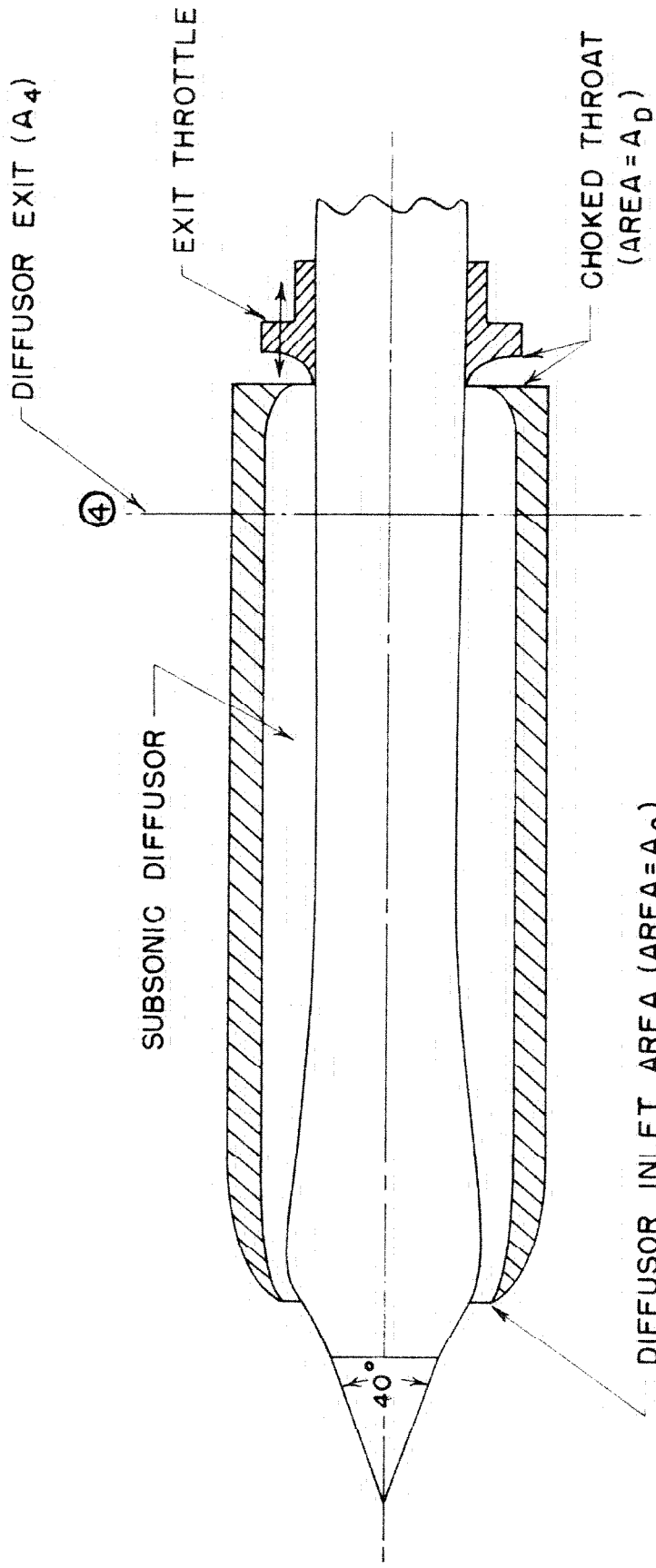

FIG. I — SCALE DRAWING OF OSWATITSCH'S DIFFUSOR

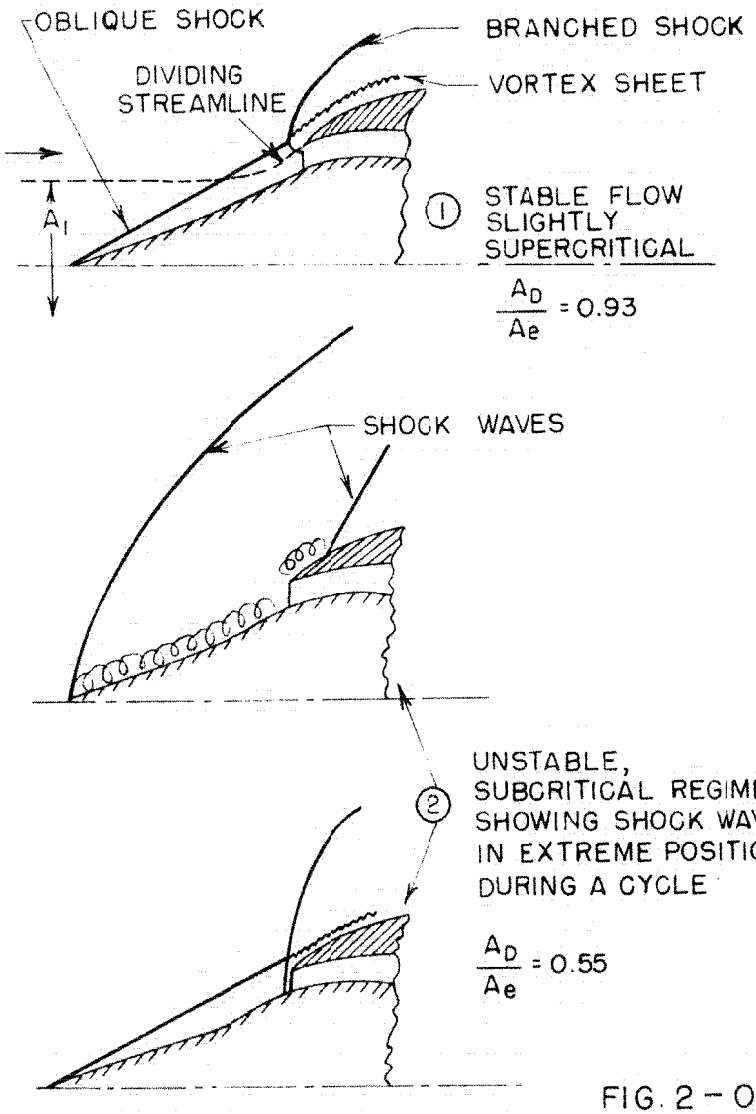

(b) REPRODUCTION OF SCHLIEREN PHOTOS

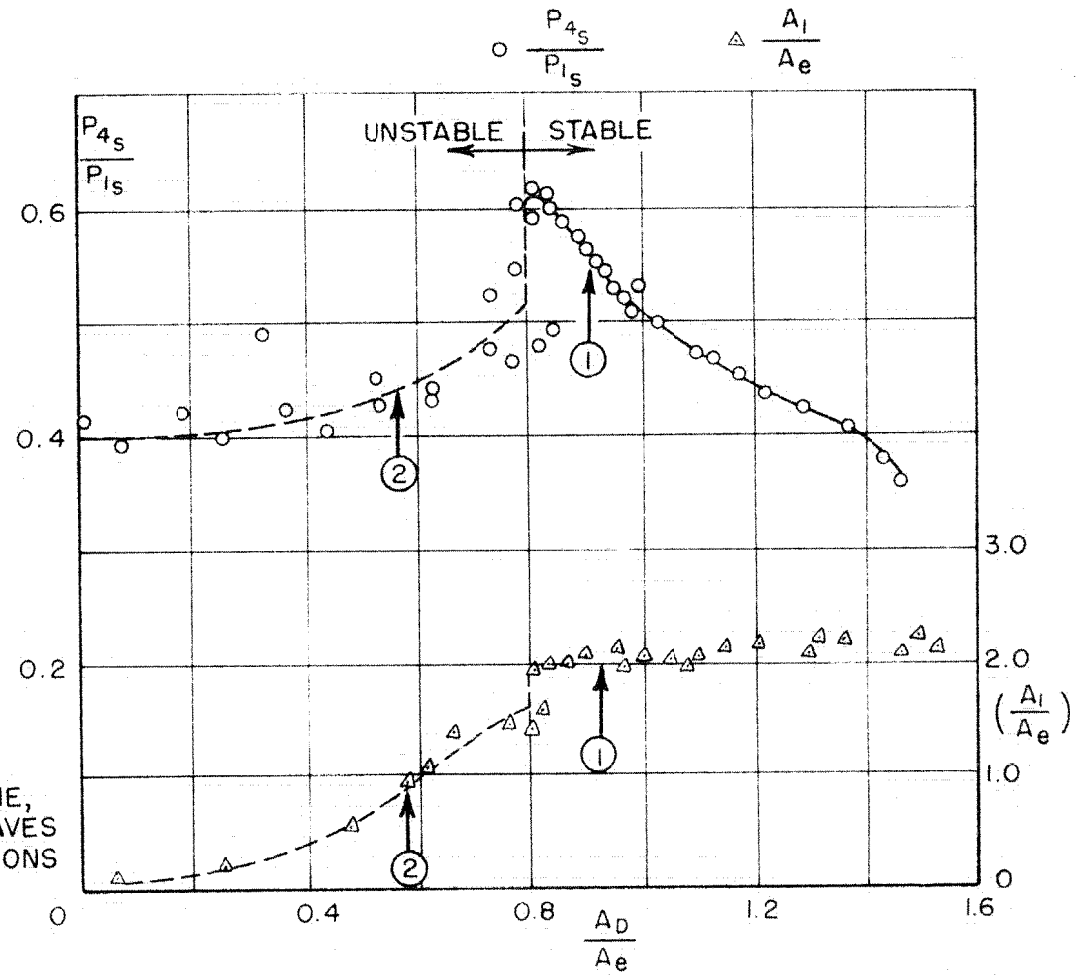

(a) PRESSURE RECOVERY AND MASS FLOW PERFORMANCE

FIG. 2 – OSWATITSCH DIFFUSOR PERFORMANCE ILLUSTRATING TRANSITION TO UNSTABLE FLOW, M = 2.9 (DATA FROM REF. 1)

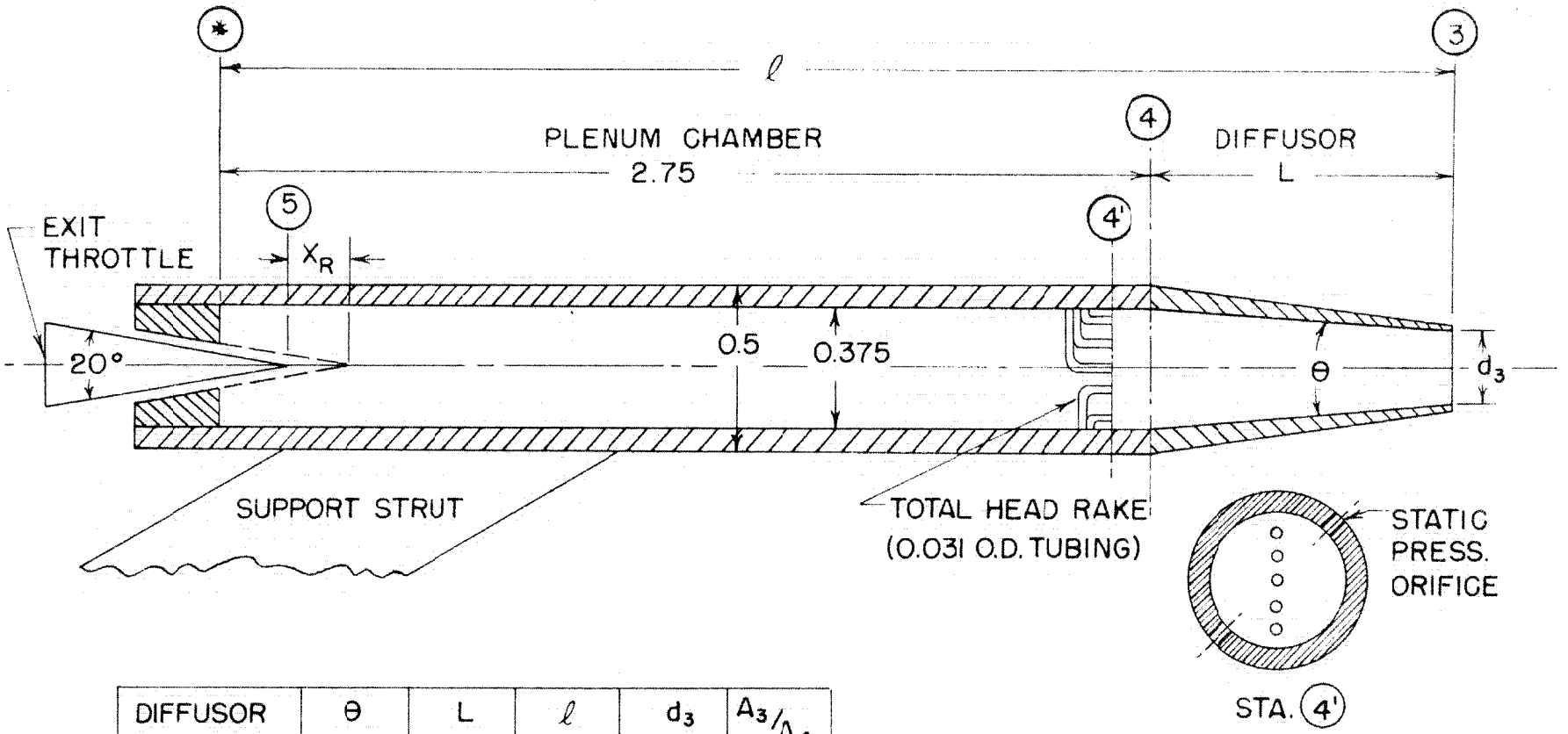

DIFFUSOR NOTATION	θ (deg.)	L (in.)	ℓ (in.)	d_3 (in.)	A_3/A_4
D_1	10	0.647	3.397	0.268	0.510
D_2	"	0.925	3.675	0.227	0.366
D_3	"	1.062	3.812	0.199	0.282
D_5	0	0.925	3.675	0.375	1.0

NOTE:
1. SCALE: TWICE
2. ALL DIMENSIONS IN INCHES

FIG. 3 – SUPERSONIC DIFFUSOR MODEL

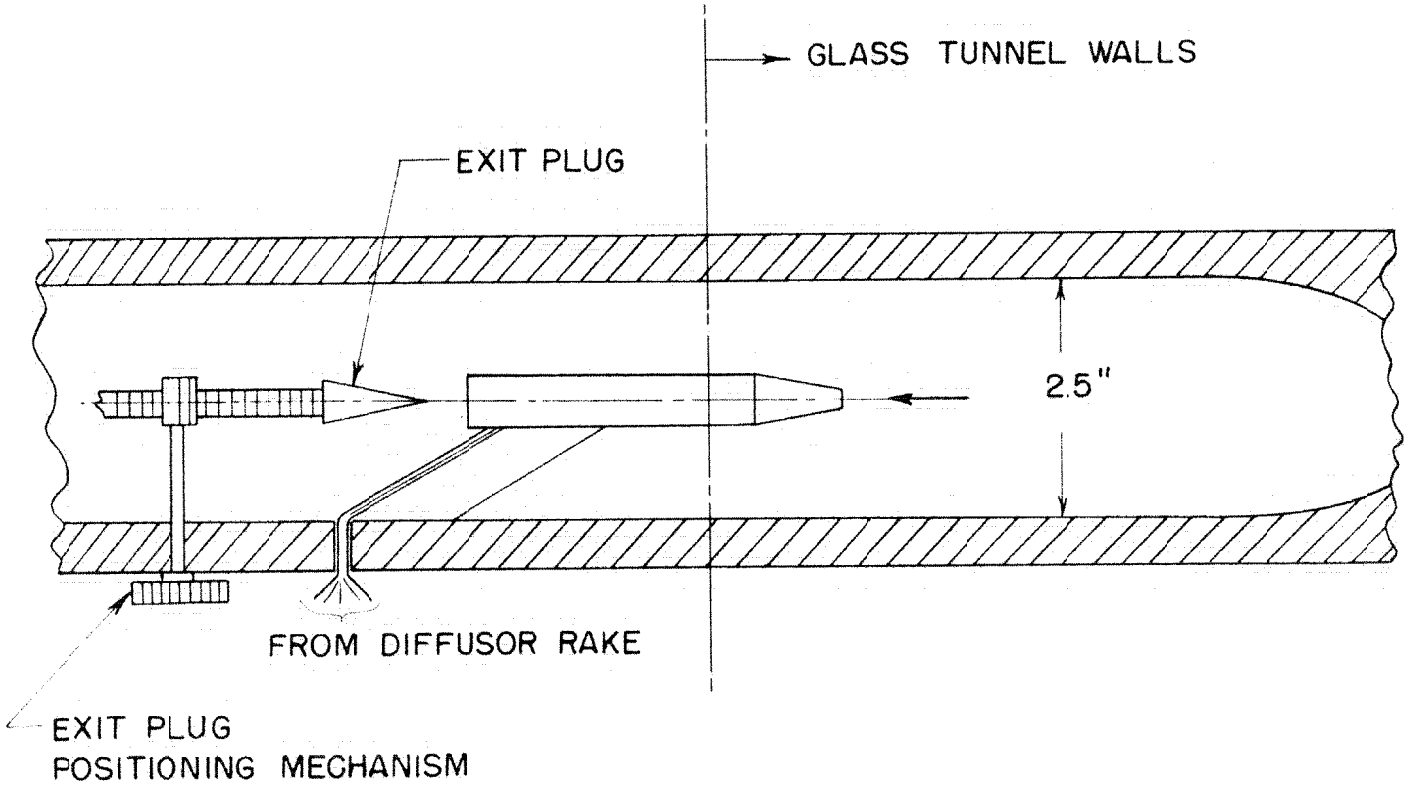

FIG. 4 – DIFFUSOR MODEL INSTALLATION IN A GALCIT 2.5" SUPERSONIC WIND TUNNEL

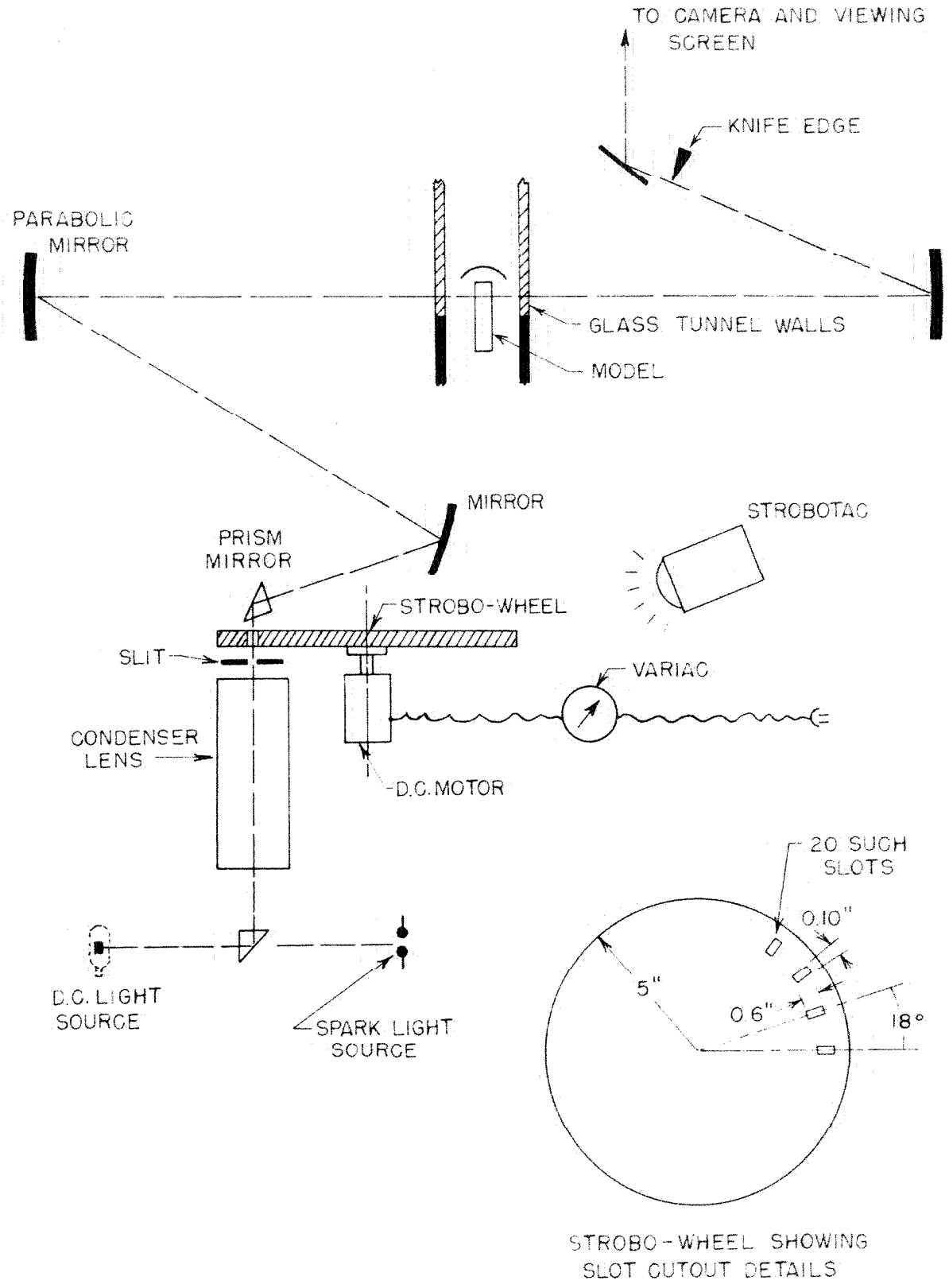

FIG. 5 — DIAGRAMMATIC SKETCH SHOWING SCHLIEREN AND SCHLIEREN-STROBOTAC SYSTEM FOR THE 2.5" GALCIT SUPERSONIC WIND TUNNEL

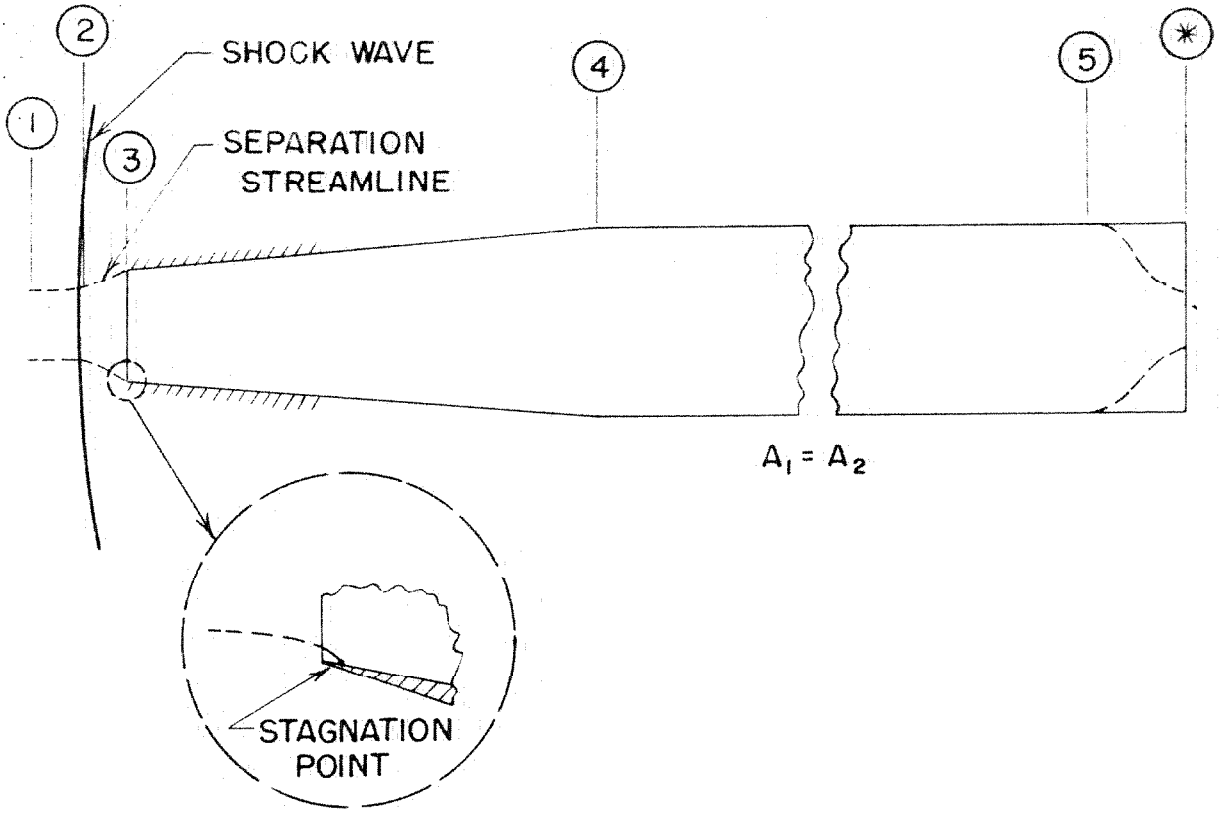

FIG. 6 – DIFFUSOR GEOMETRIC AND FLOW NOMENCLATURE

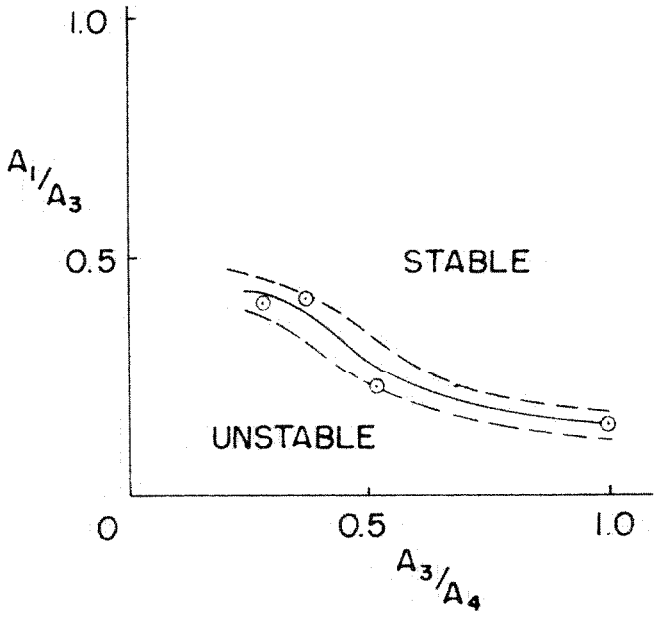

FIG. 7 - STABILITY LIMIT AS A FUNCTION OF MASS FLOW AND DIFFUSOR GEOMETRY, $M_1 = 2$

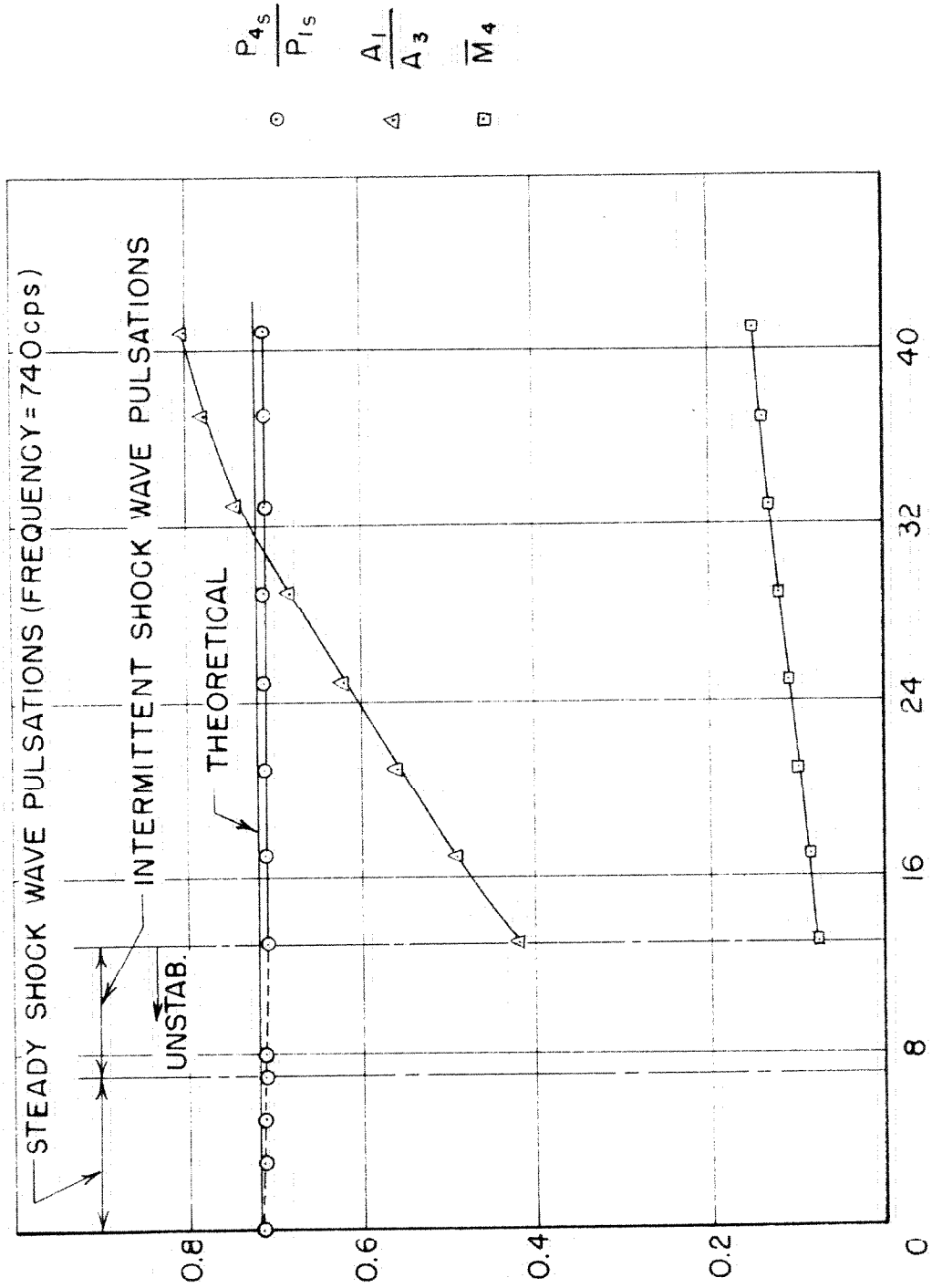

FIG. 8 – DIFFUSOR D_2 PERFORMANCE, $M_1 = 2.0$

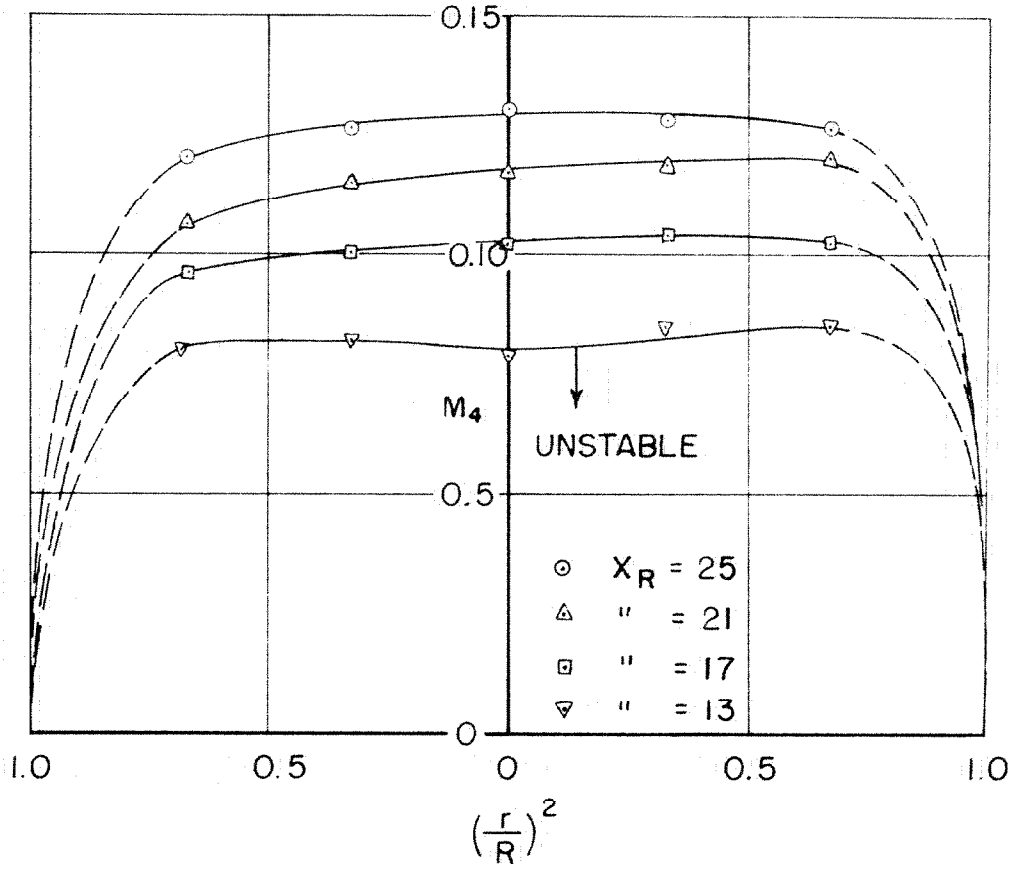

FIG. 9 – VELOCITY PROFILES AT DIFFUSOR EXIT FOR SUBCRITICAL FLOW PRECEDING INSTABILITY; DIFFUSOR D_2, $M_1 = 2.0$

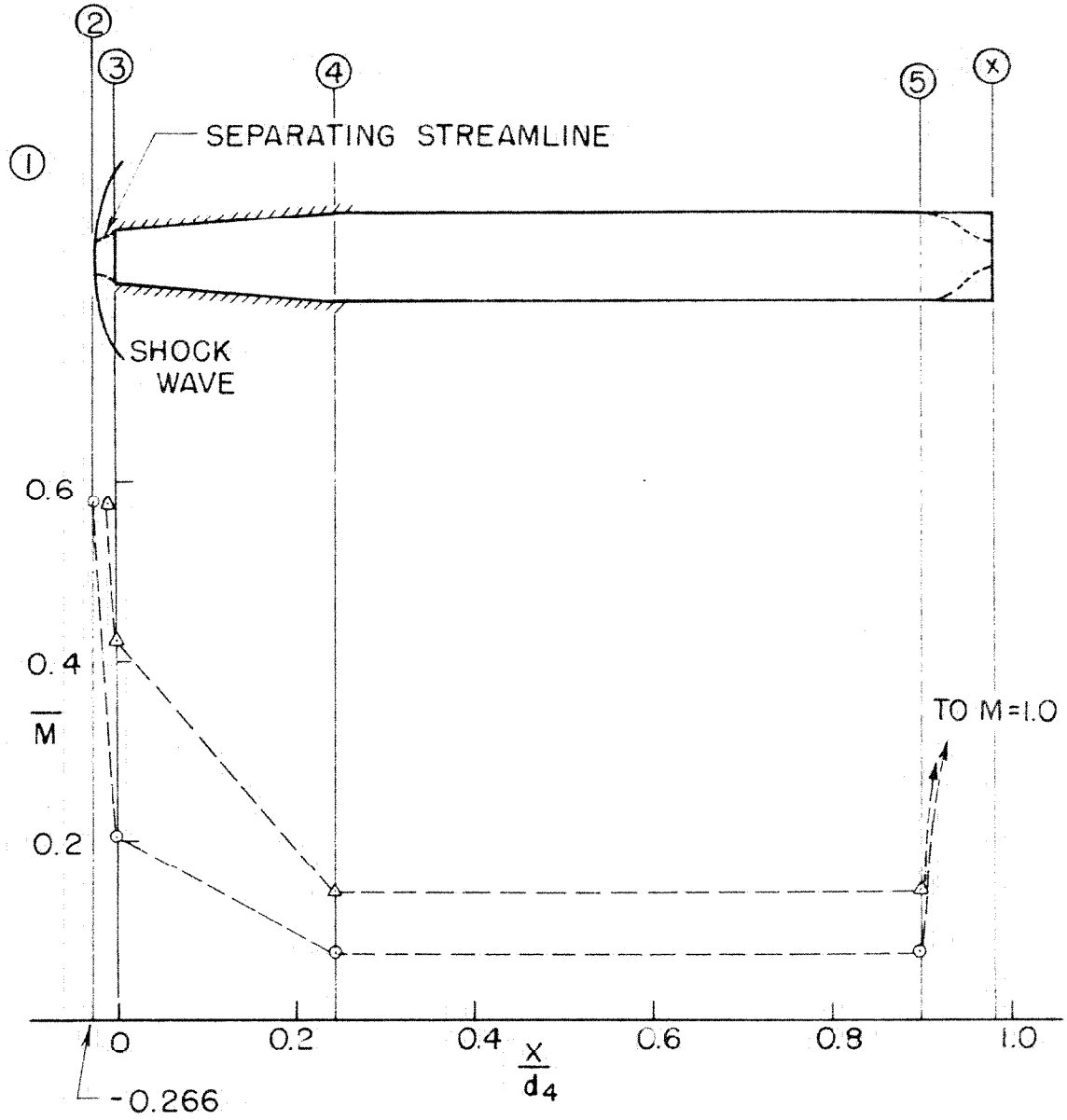

FIG. 10 - AXIAL VELOCITY DISTRIBUTION JUST PRECEDING INSTABILITY, DIFFUSOR D_2, M_1 = 2.0

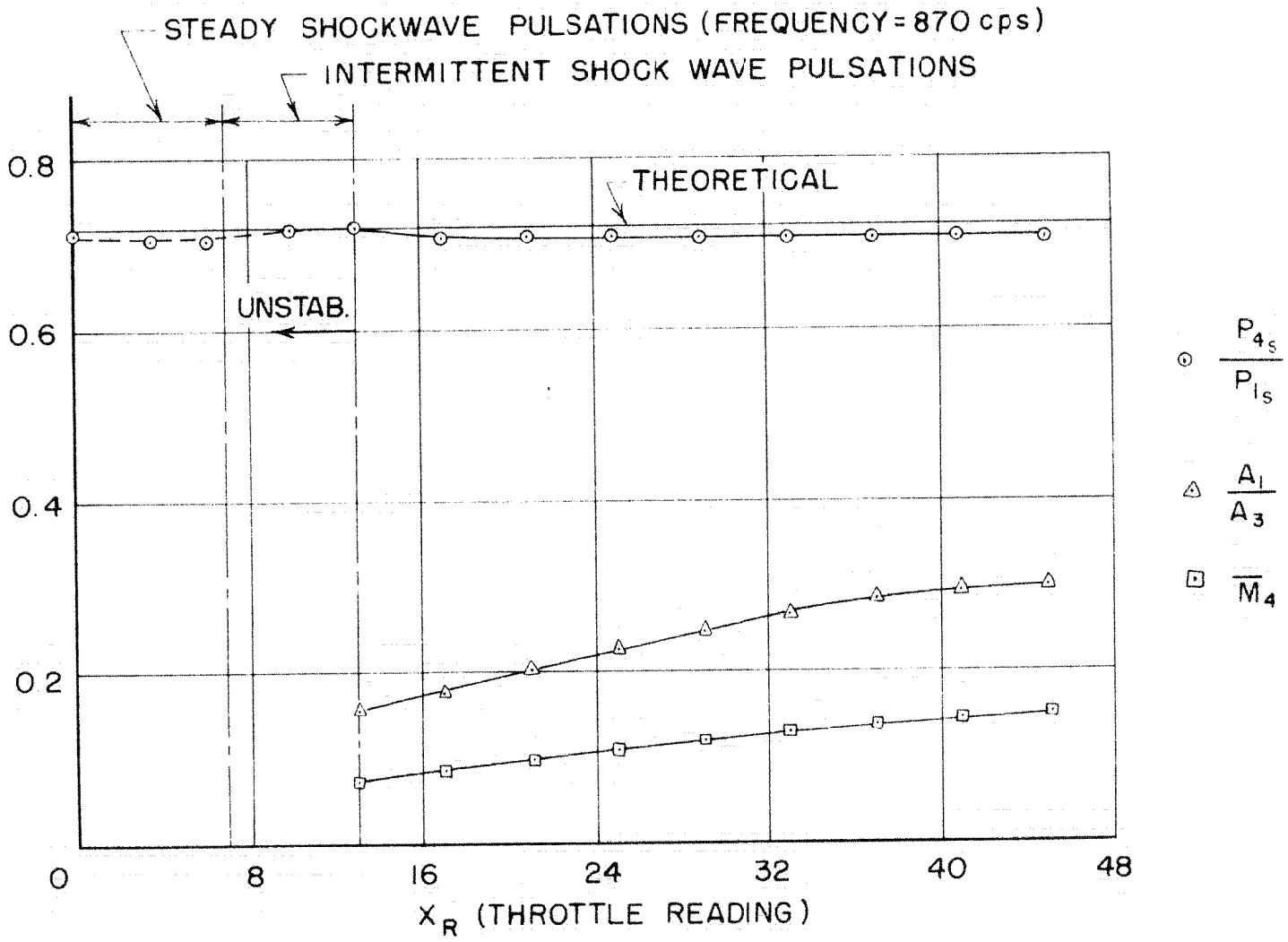

FIG. 11 – DIFFUSOR D_5 PERFORMANCE, $M_1 = 2.0$

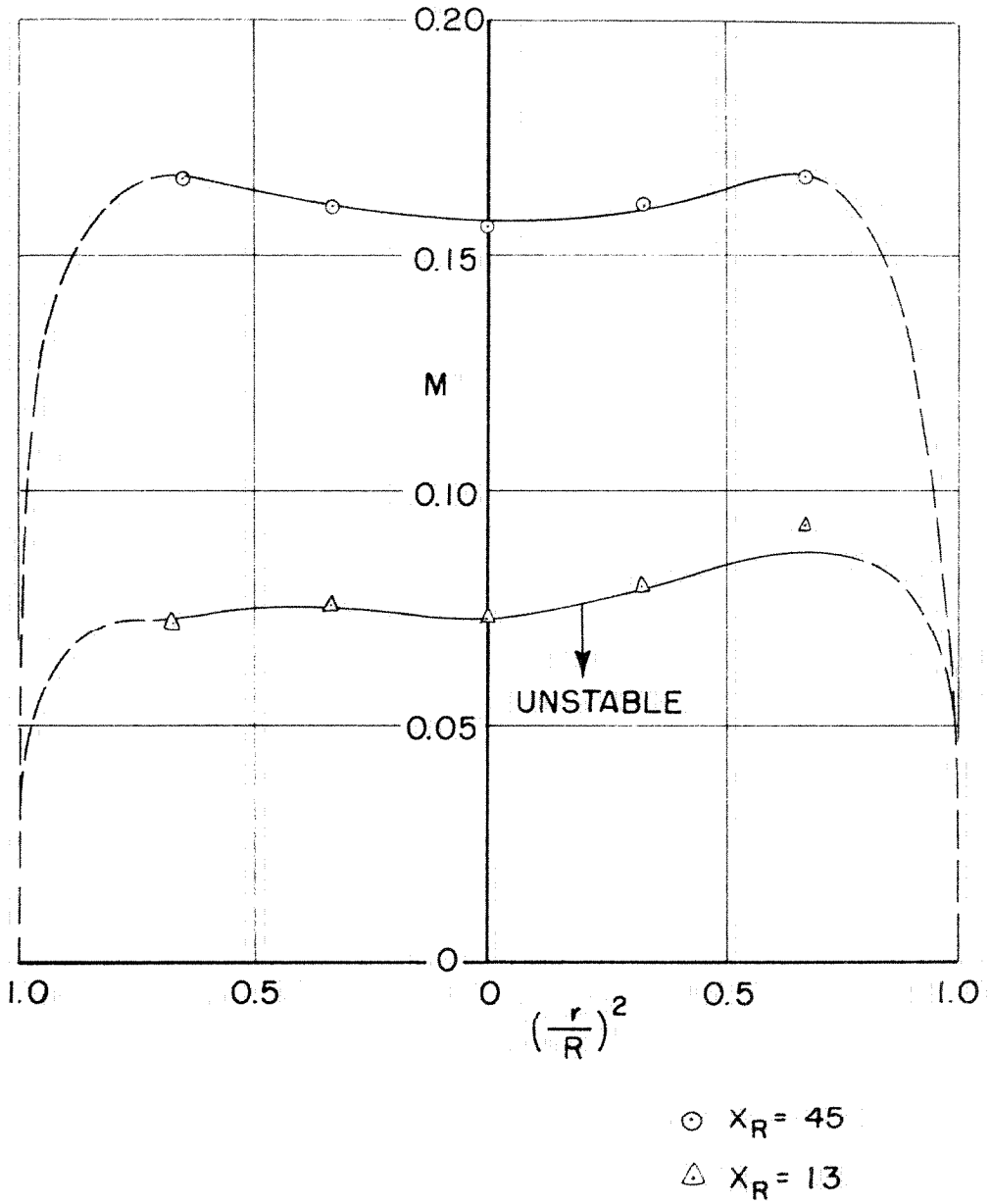

FIG. 12 - VELOCITY PROFILES AT DIFFUSOR EXIT FOR SUBCRITICAL FLOW PRECEDING INSTABILITY, DIFFUSOR D_5, M_1 = 2.0

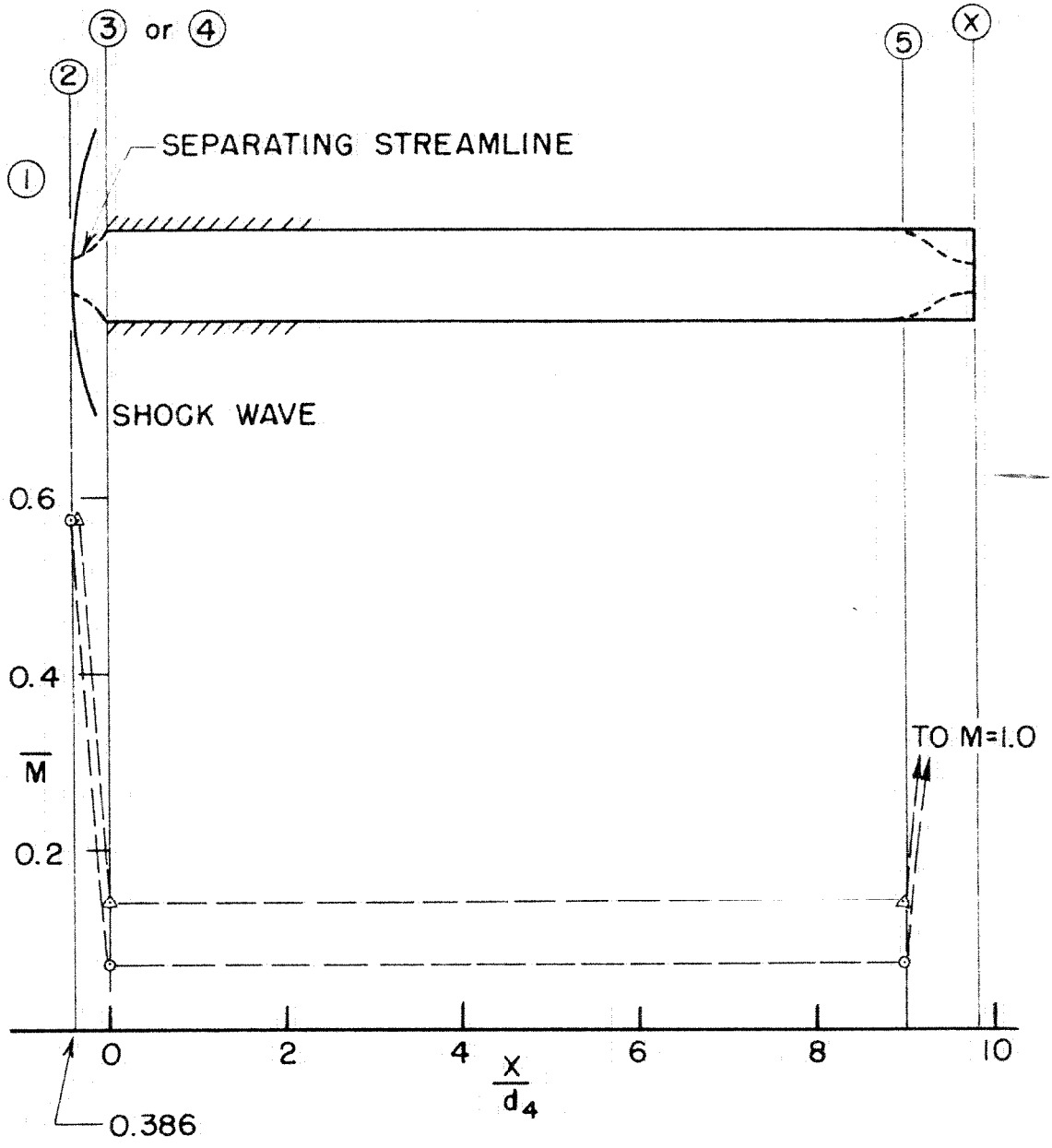

△ SUBCRITICAL, $A_1/A_3 = 0.30$, $X_R = 45$

⊙ JUST PRECEDING INSTABILITY, $A_1/A_3 = 0.16$, $X_R = 13$

FIG. 13 – AXIAL VELOCITY DISTRIBUTION JUST PRECEDING INSTABILITY, DIFFUSOR D_5, $M_1 = 2.0$

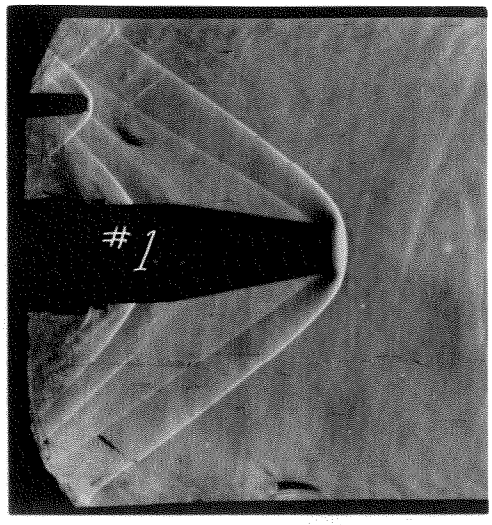

(a) x_R = 13, A_1/A_3 = 0.42, Steady Exposure, Subcritical, Just Preceding Instability

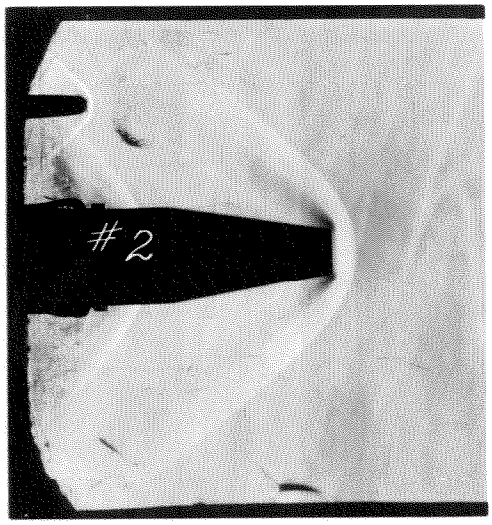

(b) x_R = 7, Steady Exposure, Unstable, Inlet Shock Pulsating at f = 740 cps, Note Limits of Shock Wave Movement

FIGURE 14 a, b -- SCHLIEREN PHOTOGRAPHS OF DIFFUSOR D_2 INLET FLOW CONDITIONS AT M_1 = 2.0: TRANSITION TO NON-STEADY FLOW

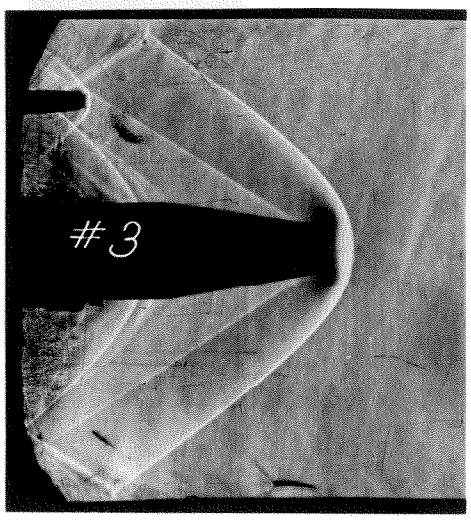

(c)

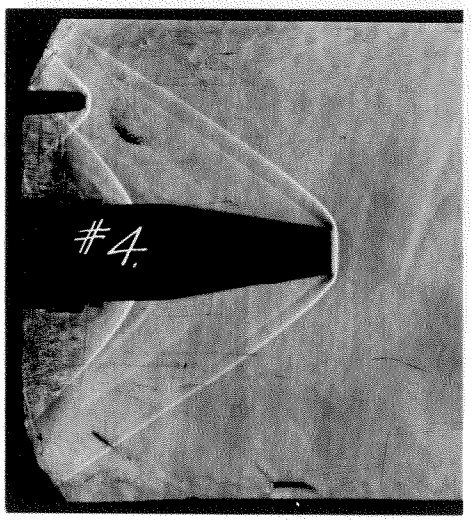

(d)

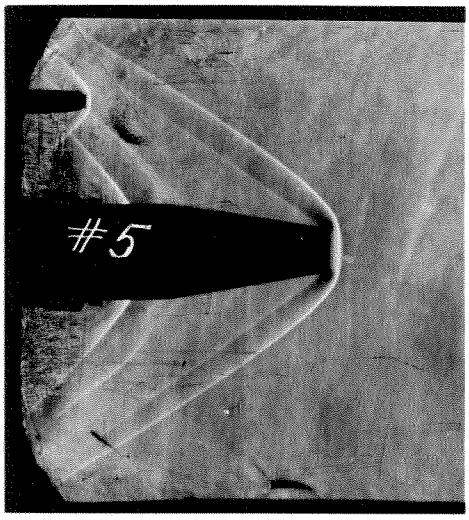

(e)

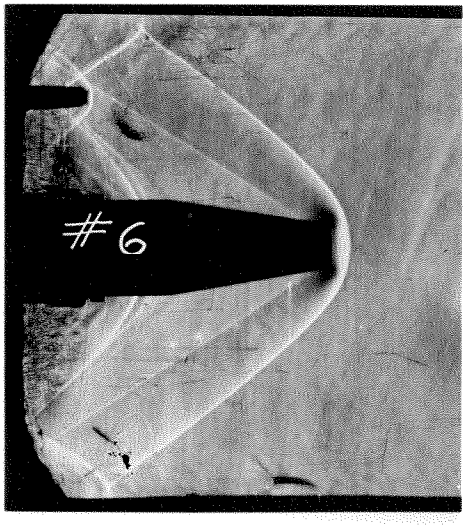

(f)

FIGURE 14 c - f -- SCHLIEREN PHOTOGRAPHS OF DIFFUSOR D_2 INLET FLOW CONDITIONS AT M_1 = 2.0: FLASH EXPOSURES SHOWING SHOCK WAVE MOVEMENT DURING A CYCLE, x_R = 7

(g) Steady Exposure, Note Enlarged Limits of Shock Wave Movement, f = 740 cps

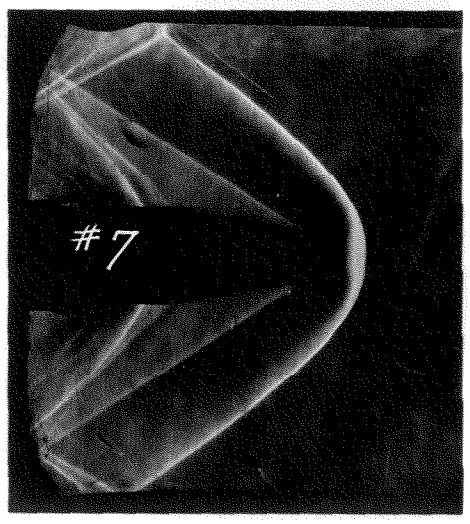

(h) Flash Exposure, Shock at Forward Limit

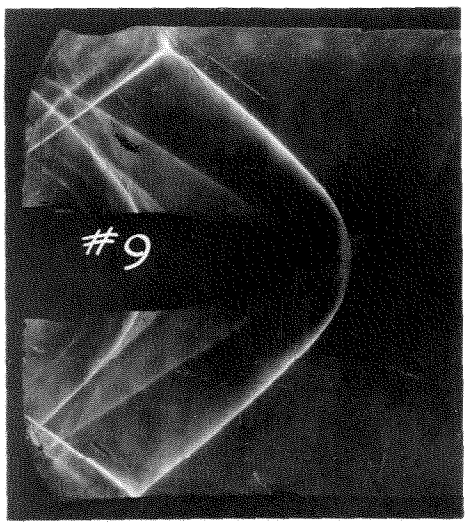

(i) Flash Exposure, Shock at Mid Position

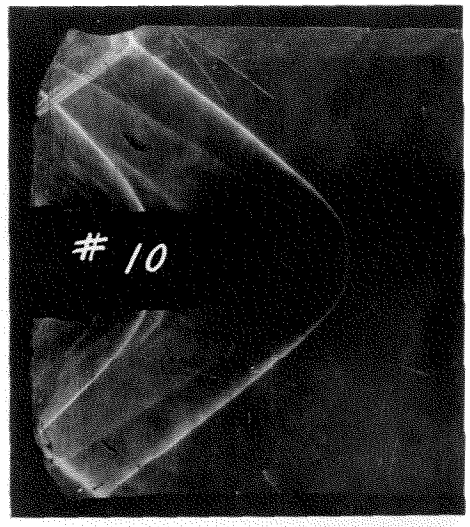

(j) Flash Exposure, Shock at Aft Limit

FIGURE 14 g - j -- SCHLIEREN PHOTOGRAPHS OF DIFFUSOR D_2 INLET FLOW CONDITIONS AT M_1 = 2.0: SHOCK WAVE MOVEMENT DURING NON-STEADY FLOW CYCLE, x_R = 0 (NO NET FLOW THROUGH DIFFUSOR)

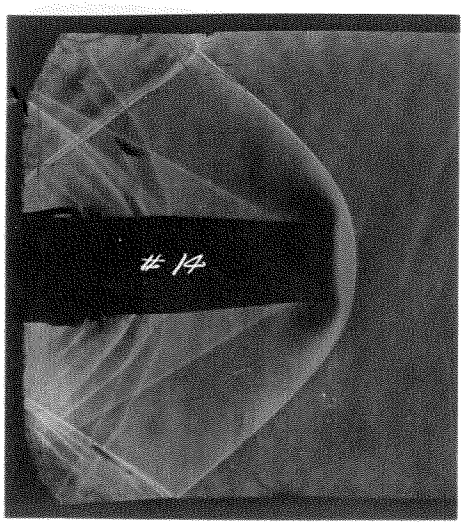

(a) x_R = 13, Steady Exposure, Subcritical, Just Preceding Instability

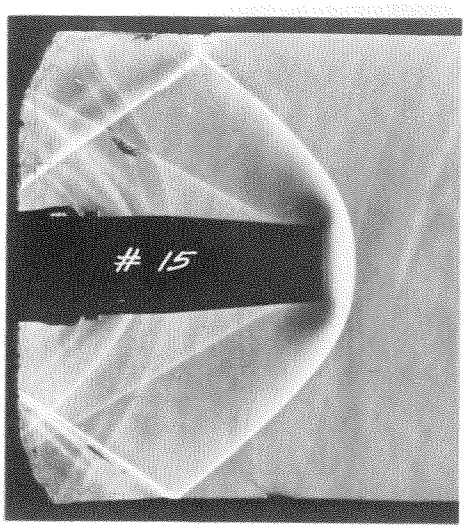

(b) x_R = 7, Steady Exposure, Unstable, Inlet Shock Pulsating at f = 870 cps, Note Shock Wave Movement

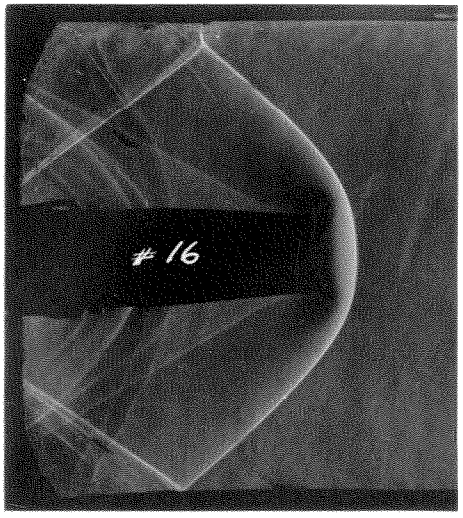

(c) x_R = 5, Flash Exposure, Shock at Forward Limit

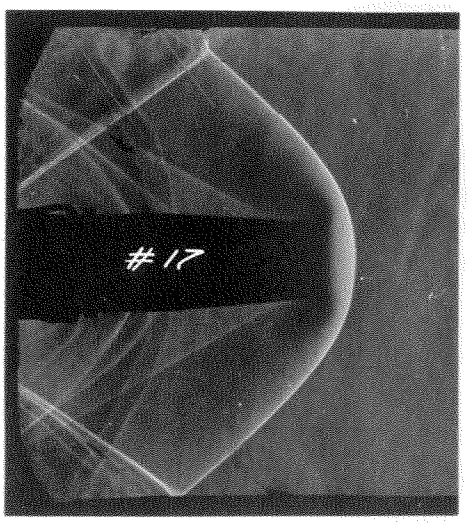

(d) x_R = 5, Flash Exposure, Shock at Aft Limit

FIGURE 15 a - d -- SCHLIEREN PHOTOGRAPHS OF DIFFUSOR D_5 INLET FLOW CONDITIONS AT M_1 = 2.0: TRANSITION TO NON-STEADY FLOW

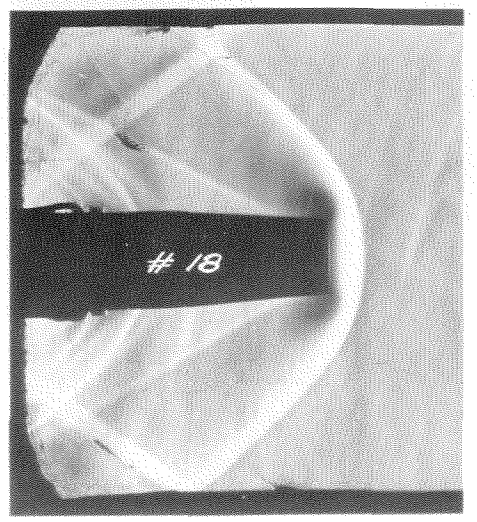

(e) Steady Exposure, Note Enlarged Limits of Shock Wave Movement f = 870 cps

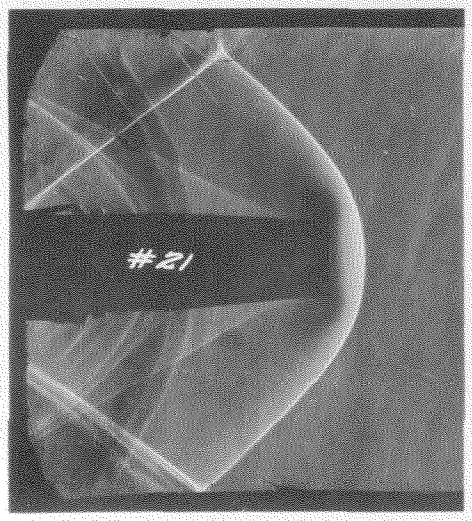

(f) Flash Exposure, Shock at Forward Limit

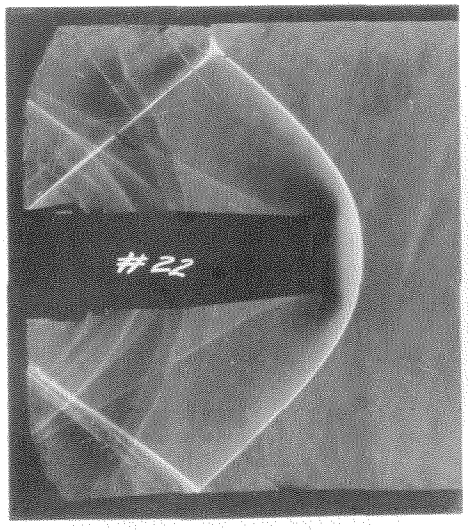

(g) Flash Exposure, Shock at Mid Position

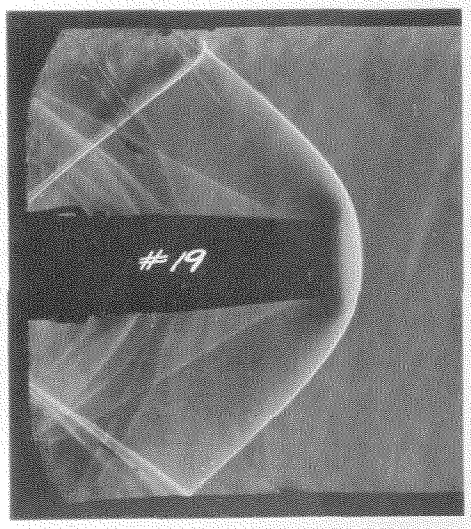

(h) Flash Exposure, Shock at Aft Limit

FIGURE 15 e - h -- SCHLIEREN PHOTOGRAPHS OF DIFFUSOR D_5 INLET FLOW CONDITIONS AT M_1 = 2.0: SHOCK WAVE MOVEMENT DURING NON-STEADY FLOW CYCLE, x_R = 0 (NO NET FLOW THROUGH DIFFUSOR)

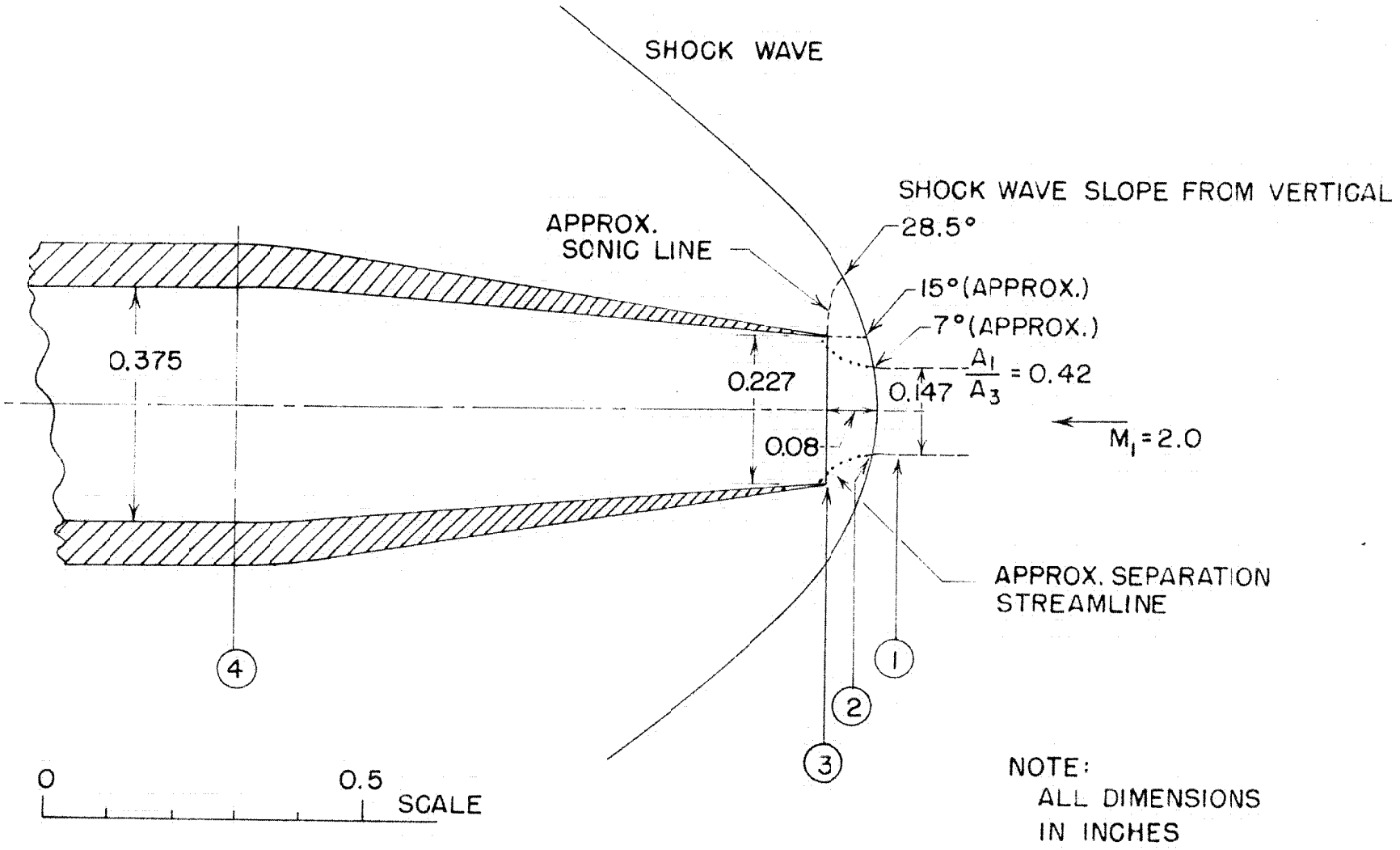

FIG. 16 – INLET FLOW DETAILS JUST PRECEDING INSTABILITY FOR DIFFUSOR D_2 (FROM ENLARGEMENT OF FIG. 14a)

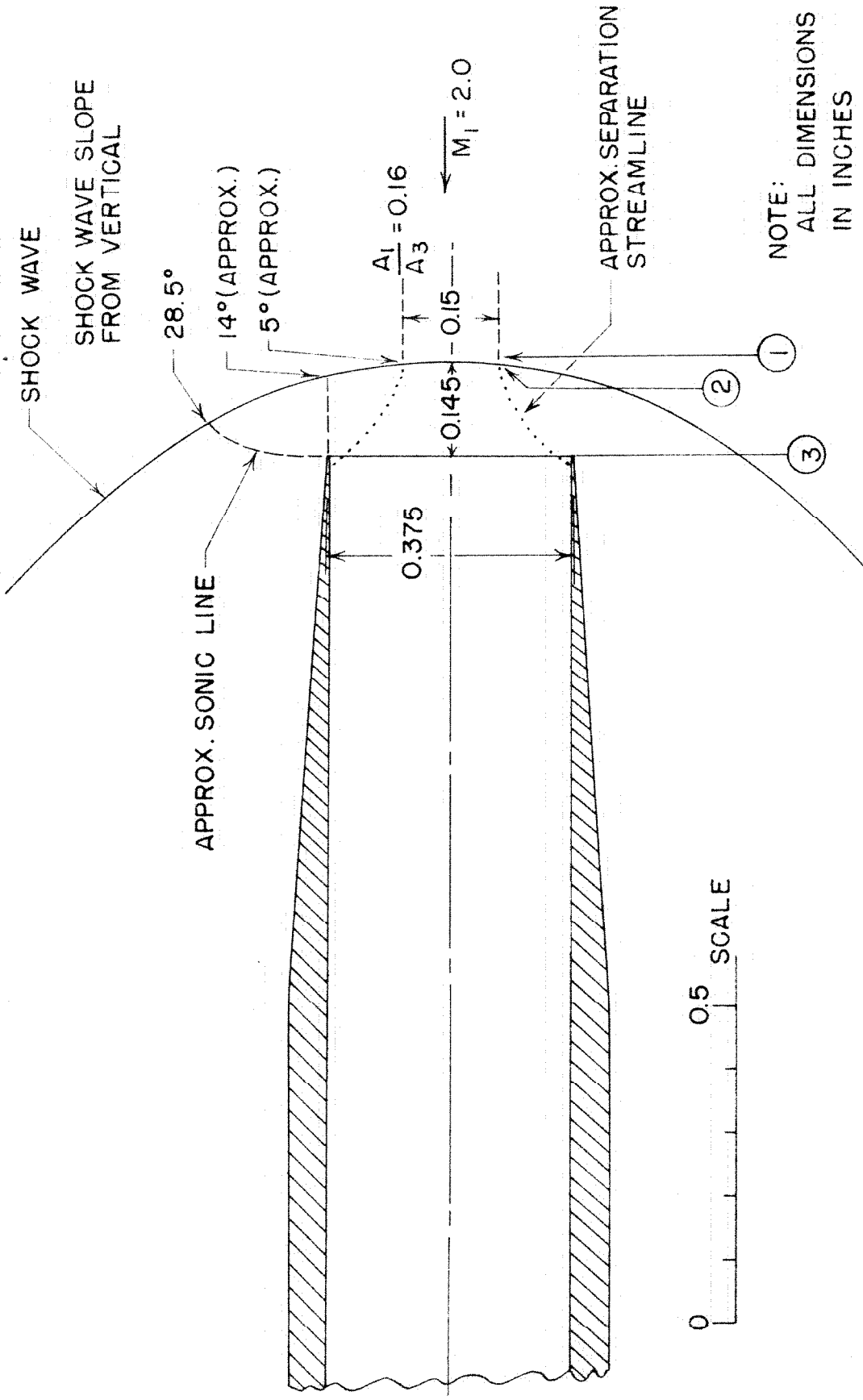

FIG. 17 – INLET FLOW DETAILS JUST PRECEDING INSTABILITY FOR DIFFUSOR D_5 (FROM ENLARGEMENT OF FIG. 15a)

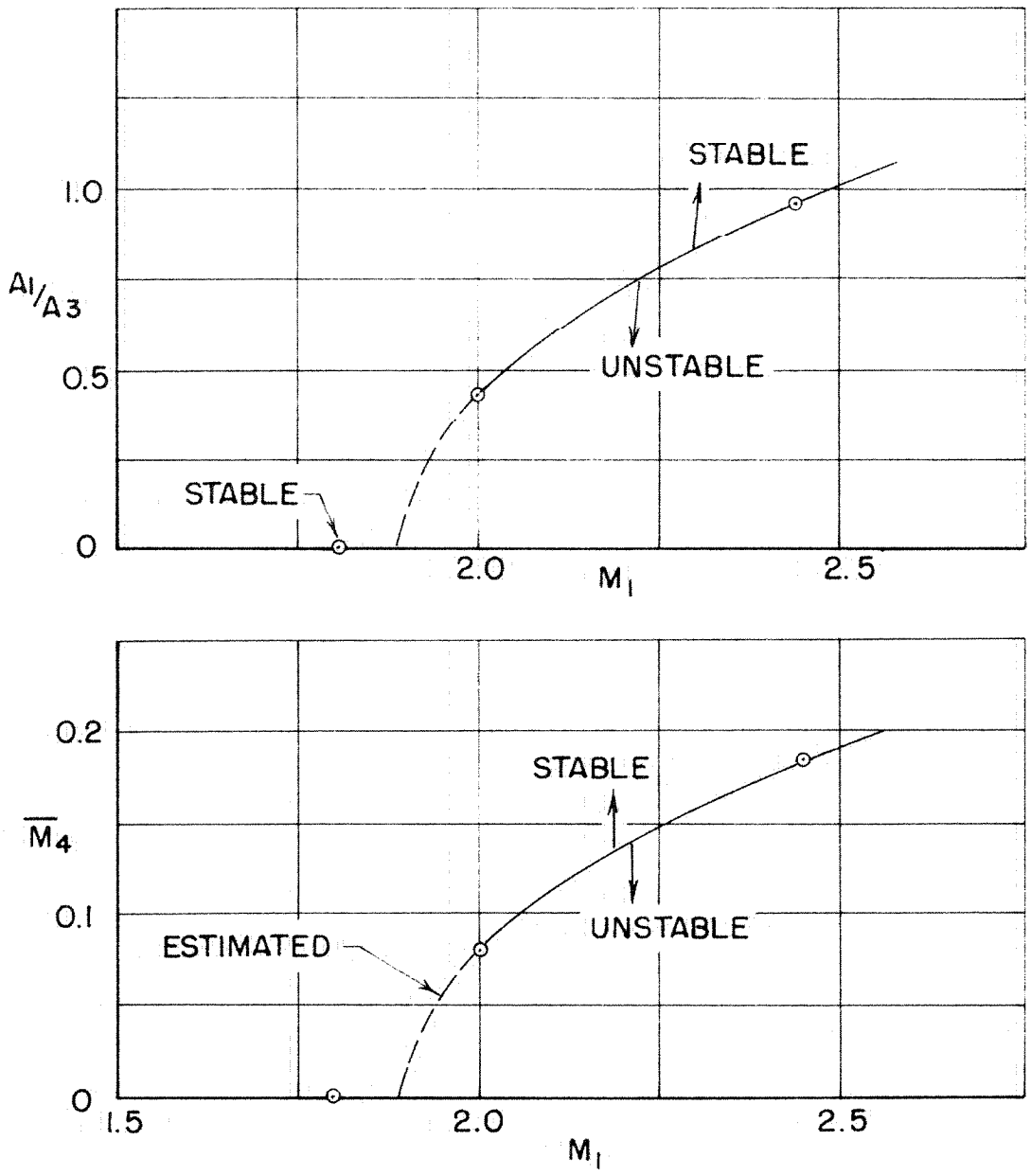

FIG. 18 – EFFECT OF FREE STREAM MACH NUMBER ON STABILITY, DIFFUSOR D2

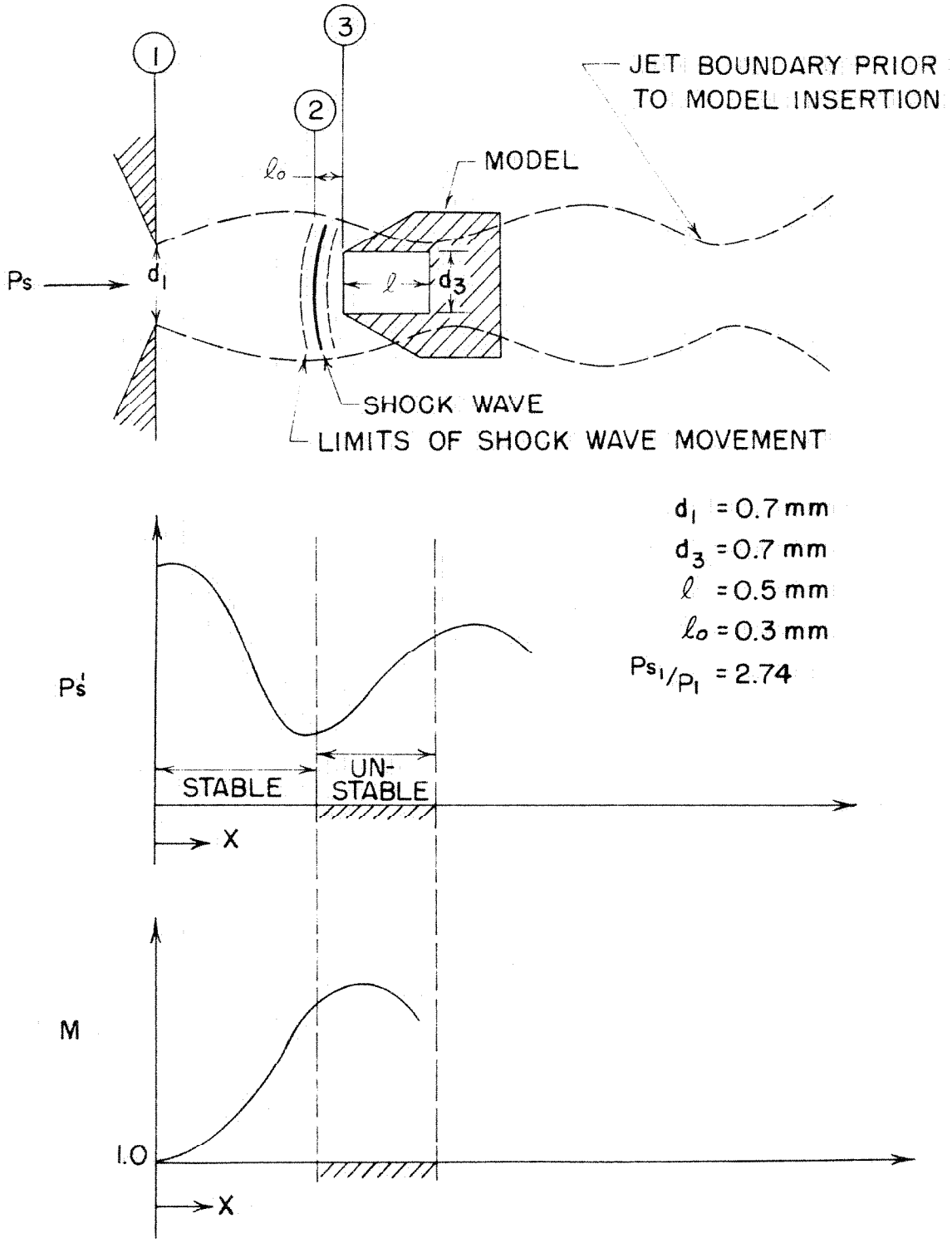

FIG. 19 - CHARACTERISTICS OF THE HARTMANN SOUND GENERATOR

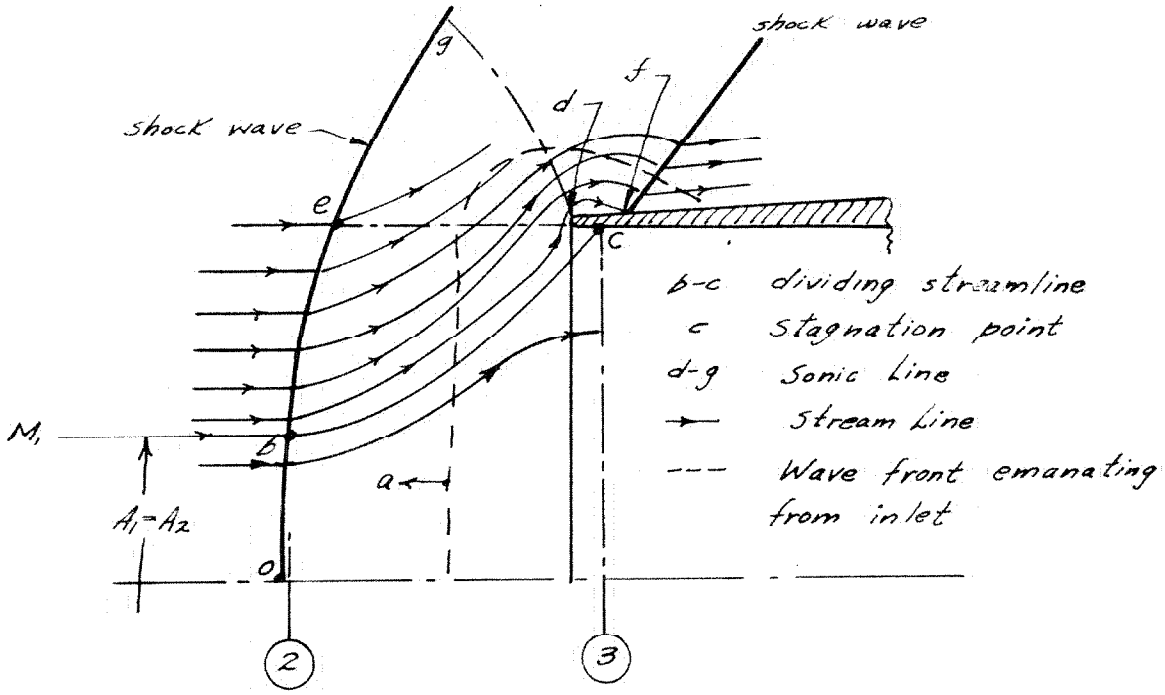

(a) Estimated Flow Field in External Diffusion Regime

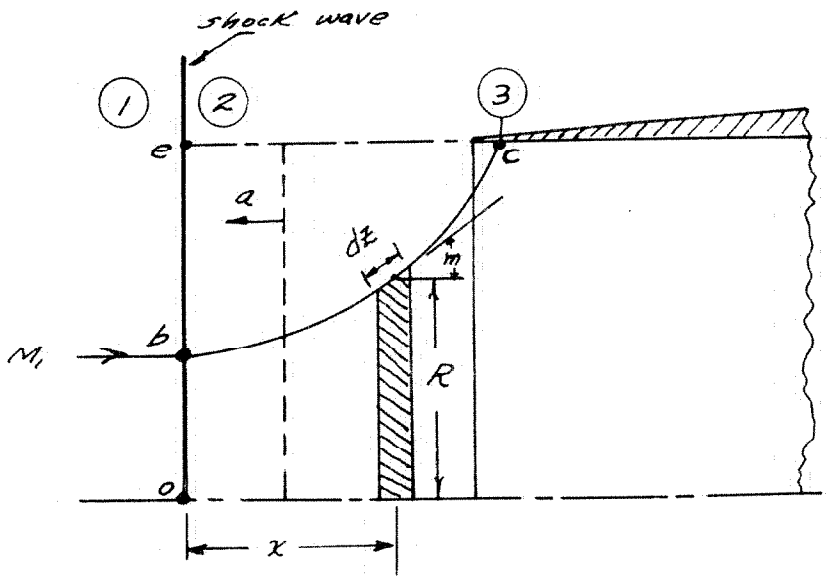

(b) Postulated Theoretical Model

FIG. 20 EXTERNAL DIFFUSION FLOW FIELD JUST PRECEDING INSTABILITY, DIFFUSOR D_5, $M_1 = 2.0$

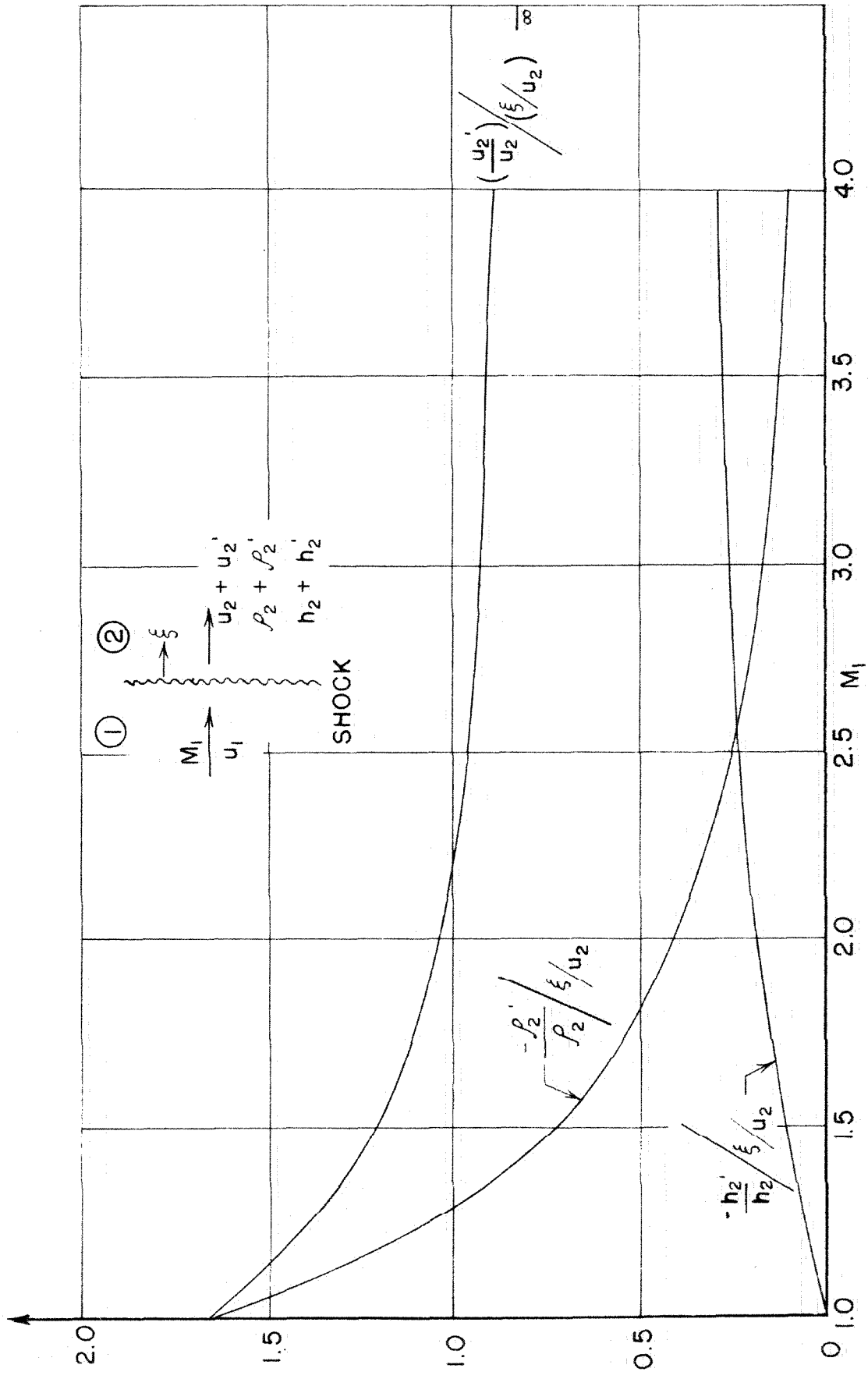

FIG.21 – LINEARIZED PERTURBATION QUANTITIES BEHIND A NON STEADY NORMAL SHOCK

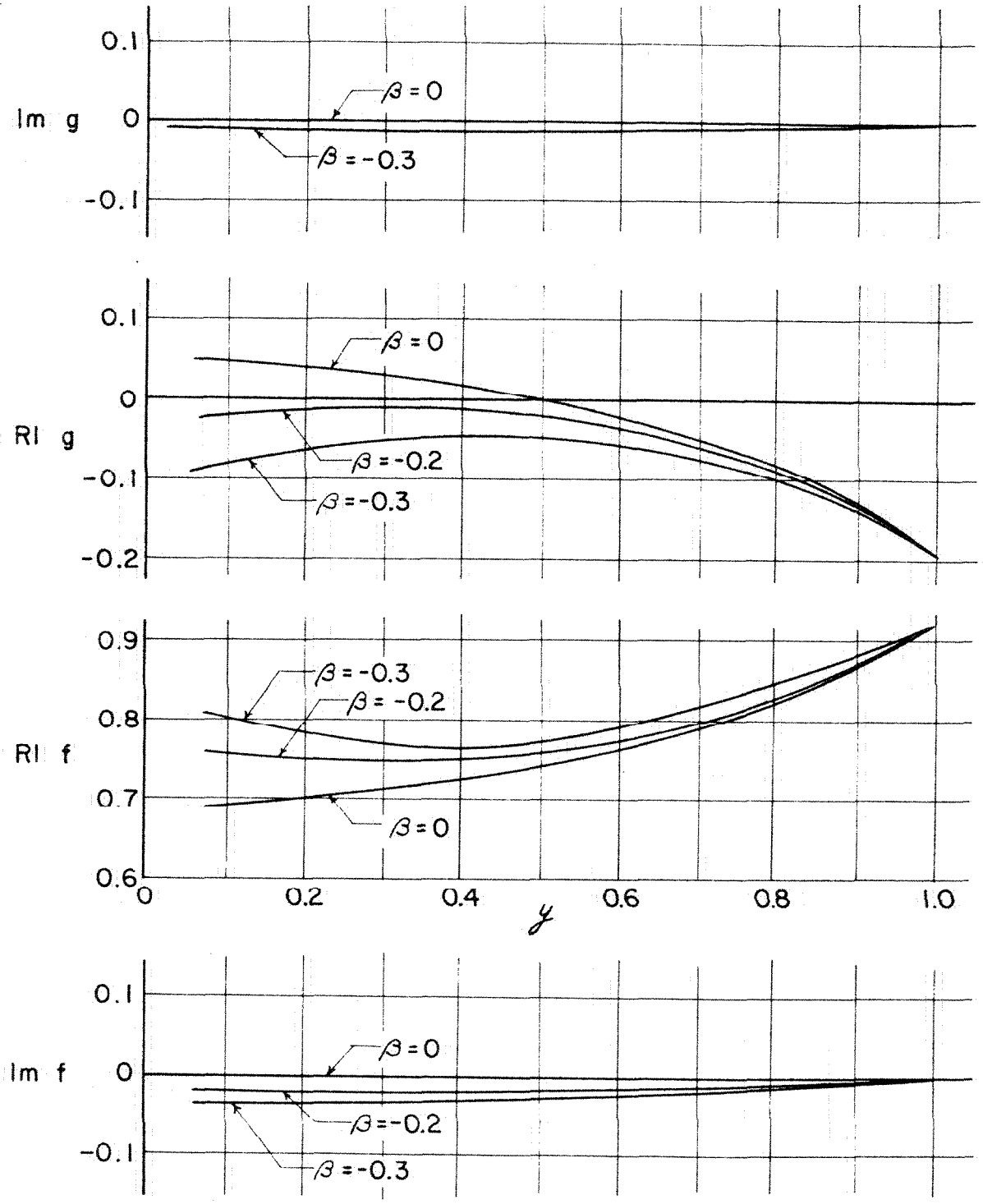

FIG. 22 EFFECT OF REDUCED FREQUENCY, $M_1 = 3.0$

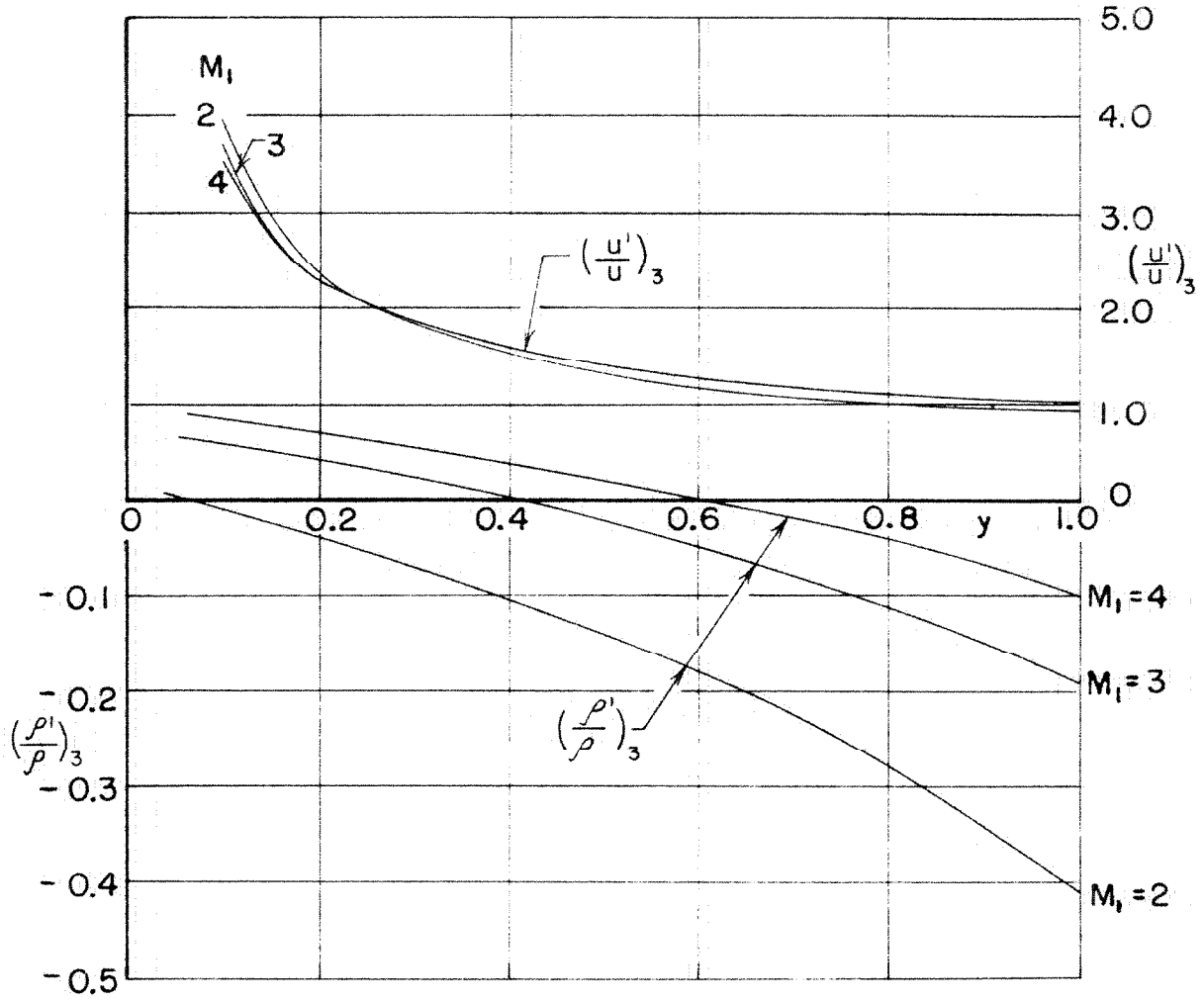

FIG. 23 – DENSITY AND VELOCITY PERTURBATIONS AT DIFFUSOR INLET FOR QUASI STEADY FLOW IN EXTERNAL DIFFUSION REGIME

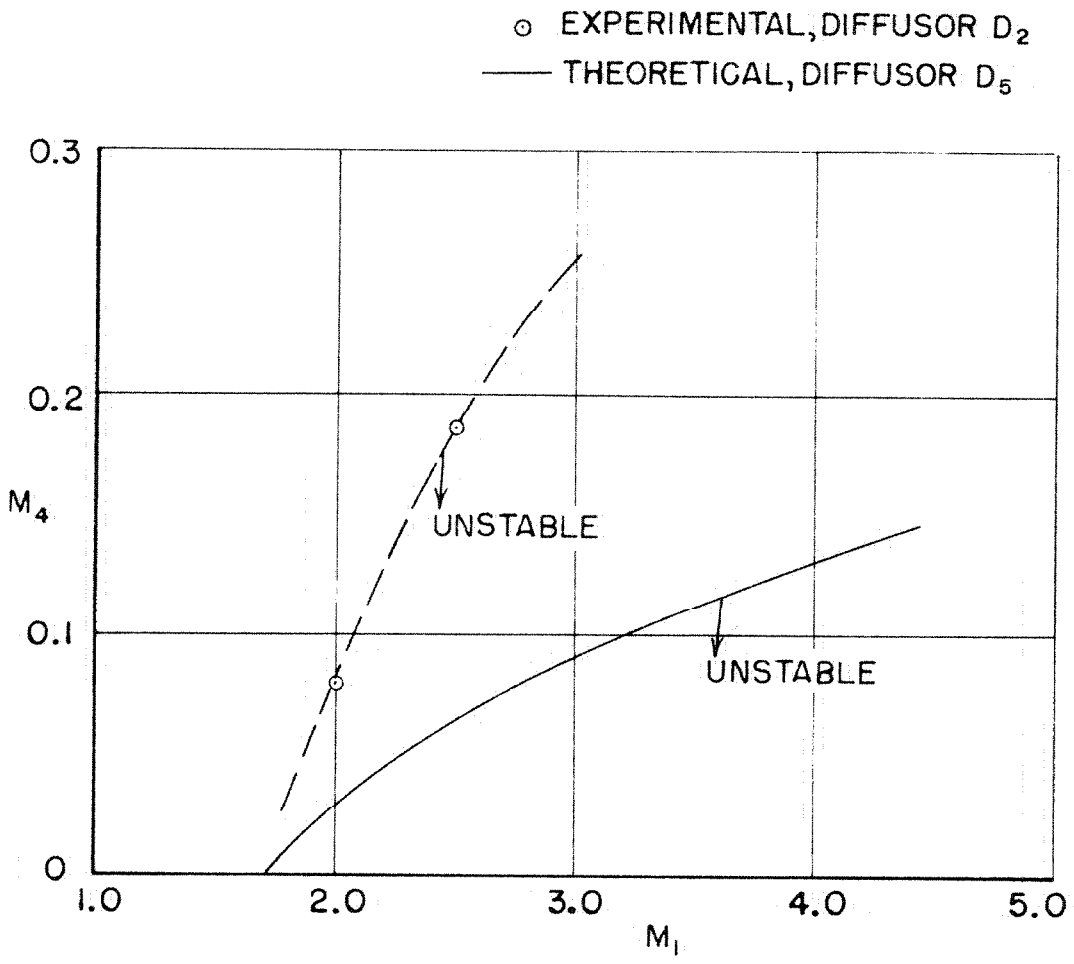

FIG. 24 - EXPERIMENTAL AND THEORETICAL STABILITY BOUNDARIES